Characterization of a Novel Protein – 3D10 – a Secreted Receptor Form of the Human Osteoclast-Associated Receptor (OSCAR)

Emad Ali Khan

A dissertation submitted to the faculty of the University of North Carolina at Chapel Hill in partial fulfillment of the requirements for the degree of Doctor of Philosophy in the School of Dentistry (Curriculum in Oral Biology)

Chapel Hill

2007

Approved by:

Advisor: Dr. Patrick Flood

Reader: Dr. Ikramuddin Aukhil

Reader: Dr. Cai-Bin Cui

Reader: Dr. Eric Everett

Reader: Dr. Luda Diatchenko

ABSTRACT

EMAD ALI KHAN: Characterization of a Novel Protein – 3D10 – a Secreted Receptor Form of the Human Osteoclast-Associated Receptor (OSCAR)
(Under the direction of Dr. Patrick Flood)

Human osteoclast-associated receptor (hOSCAR) is a member of the leukocyte receptor cluster (LRC) of an unknown ligand. hOSCAR has been reported to be expressed in several mononuclear cells (MNC) of myeloid origin and plays a role in modulating innate and adaptive immune response. We identified an alternative spliced isoform of hOSCAR that we named 3D10. Sequence analysis showed that 3D10 is one of a group of hOSCAR with a non-spliced intron resulting in larger transcripts and soluble proteins lacking a trans-membrane domain. Comparisons were made in tissue distribution between the two groups using specific PCR primers and rabbit polyclonal anti-hOSCAR and anti-soluble hOSCAR antibodies. Both groups were found to be differentially expressed in peripheral blood leukocytes and in a wide variety of tissues. They were also found to be expressed in all MNC and neutrophils. The membrane-bound isoforms were down-regulated more than the soluble isoforms following stimulation in MNC with the mitogens PWM, Con A and PHA. Studies using THP-1 cells showed that the soluble isoforms are up-regulated by both PMA and LPS, and that they are secreted and may act as decoy receptors. Performing yeast two hybrid screening of macrophage cDNA library identified potential binding partners that might include hOSCAR ligand and cytoplasmic modulators. Screening mouse tissues with anti-soluble hOSCAR Ab suggests the existence of the soluble group of mOSCAR. Finally,

although 3D10 has been found to be secreted, over-expressed intra-cellular 3D10 inhibits NF-κB in a TNF-α-independent pathway.

To my parents, for their unconditional love, blessings and support

And

To my wife, for her motivation, encouragement and support and for her patience being with three children and away from her parents

ACKNOWLEDGEMENTS

I would like to acknowledge all the people, laboratories, facilities and institutions who supported this project.

Special thanks and specific acknowledgements go to the following:

The Dental Research Center (DRC) of the School of Dentistry including all of its current and previous labs and people for sharing reagents, equipments and experience

Albert Baldwin's Lab for providing reagents for NF-κB studies

Jenny Ting's Lab for providing assistance for NF-κB studies

Lineberger Cancer Center and Tissue Culture Facility for providing different reagents, cell-lines, primers and other materials

MSL (Microscopy) for helping with immunofluorescence slides

Genome Analysis Facility for DNA sequencing

NIH for funding

King Abdulaziz University for granting the full scholarship to pursue this degree

PREFACE

"And say: "My Lord! Increase me in knowledge""

The Holy Quran, Taaha 20:114

"That Allah may reward them according to the best of their deeds, and add even more for them out of His Grace. And Allah provides without measure to whom He wills"

The Holy Quran, Annoor 24:38

"And your Lord proclaimed: "If you thank, I will give you more""

The Holy Quran, Ibraaheem 14:7

All the praise is due to Allah. He blessed me with blessings I will never be able to count. During my pursuit of this PhD degree, He blessed me with a nice group of people who expressed their help and kindness when I needed and when I did not ask for. Peace and blessing be upon our beloved prophet Mohammad, who said: "The one who does not thank the people does not thank Allah". Following his guidance, I write this acknowledgement. To all of those people I am very grateful, and I say Thank you. I'd like to recognize some people for their special support:

My dissertation advisors: Dr. Ikramuddin Aukhil and Dr. Patrick Flood, who provided me with continuous guidance and support.

My dissertation committee: Dr. Cai-Bin Cui, Dr. Eric Everett and Dr. Luda Diatchenko who provided me with valuable suggestions, advice and support.

My current and previous colleagues, faculty and staff of the oral biology program. And special thanks to Ms. Cindy Blake, the program manager.

My friends at Jamaat Ibad Ar-Rahman in Durham and at the Islamic Center of Raleigh, and the Saudi and Gulf group who made my family and me feel like home.

King Abdulaziz University, the Saudi Arabian Cultural Mission to the USA, and the government of Saudi Arabia in general for the scholarship and support.

TABLE OF CONTENTS

Page

LIST OF TABLES

Page

LIST OF FIGURES

LIST OF ABBREVIATIONS AND SYMBOLS

%	Percent (or Percentage)
<	Less Than
>	More Than
°C	Degree Celsius (or Centigrade)
^{32}P-dCTP	Phosphor 32-Labeled Deoxycytidine Triphosphate
AA	Amino Acid
Ab	Antibody
AD	Activation Domain
Ade	Adenine
Amp	Ampicillin
ANK	Ankyrin Repeats
ATCC	American Type Culture Collection
BAT3	Hla-B-Associated Transcript 3
BD	Binding Domain
bp	Base-Pair
BMD	Bone Mineral Density
BSA	Bovine Serum Albumin
cDNA	Complementary DNA
c-Fms	M-CSF Receptor
CM	Conditioned Media
cm	Centimeter
CO_2	Carbon Dioxide
Con A	Concanavalin A
CsCl	Cesium Chloride
CSF-1R	M-CSF Receptor
(number) d	(number) Day(s)
DCs	Dendritic Cells
DEPC	Diethyl Pyrocarbonate
dH_2O	Distilled Water
DMEM	Dulbecco's Modified Eagle's Medium
DMSO	Dimethyl Sulfoxide
DNA	Deoxyribonucleic Acid
DP (number)	(number order) Difference Product
ds	Double Strand
DTT	Dithiothreitol
EDTA	Ethylene Diamine Tetra-Acetic Acid
EEx3	EPPS-EDTA
EPPS	N-2-Hydroxyethylpiperazine-N'-3-Propanesulfonic Acid
EST	Expressed Sequence Tag
FBS	Fetal Bovine Serum
Fc	Fragment, Crystallizable
FCS	Fetal Calf Serum

FcαR	Fc Alpha Receptor
FITC	Fluorescein Isothiocyanate
(number) g	(number) Gram(s)
G418	Hygromycin B (or Geneticin)
GAPDH	Glyceraldehyde-3-Phosphate Dehydrogenase
GM-CSF	Granulocyte Macrophage-Colony-Stimulating Factor
(number) h	(number) Hour(s)
H_2O	Water
H_2O_2	Hydrogen Peroxide
HCl	Hydrochloric Acid
HEK	Human Embryonic Kidney
HGNC	HUGO Gene Nomenclature Committee
His	Histidine
HLA	Human Leukocyte Antigen
hOSCAR	Human OSCAR
hOSCARm	Membrane-Bound Human OSCAR
hOSCARs	Soluble (or Secreted) Human OSCAR
HUGO	Human Genome Organization
Ig	Immunoglobulin
Ig-SF	Immunoglobulin Super-Family
IKK	Iκb Kinase
IL-(number)	Interleukin-(number)
IL-1R	IL-1 Receptor
ILT	Ig-Like Transcript
IP	Immuno-Precipitation
IPTG	Isopropyl B-D-1-Thiogalactopyranoside
ITAM	Immunoreceptor Tyrosine-Based Activation Motif
ITIM	Immunoreceptor Tyrosine-Based Inhibitory Motif
IκB	NF-κb Inhibitory Protein
KAR	Killer Cell Activatory Receptor
kb	Kilo Base
kDa	Kilo Dalton
KIR	Killer Cell Inhibitory (or Ig-Like) Receptors
KLH	Keyhole Limpet Hemocyanin
LAIR	Leukocyte-Associated Ig-Like Receptor
LB	Luria Broth
LBP	LPS-Binding Protein
Leu	Leucine
LiAc	Lithium Acetate
LILR	Leukocyte Ig-Like Receptors
LILRA	Activating Leukocyte Ig-Like Receptors
LILRB	Inhibiting Leukocyte Ig-Like Receptors
LIR	Leukocyte Ig-Like Receptor
LPS	Lipopolysaccharide
LRC	Leukocyte Receptor Cluster
LTB	Lymphotoxin Beta

Luc	Luciferase
(number) M	(number) Molar
M-CSF	Macrophage-Colony-Stimulating Factor
MD-2	Myeloid Differentiation Protein-2
MHC	Major Histocompatibility Complex
min	Minute(s)
MIR	Monocyte/Macrophage (Myeloid) Inhibitory Receptor
MITF	Microphthalmia Transcription Factor
ml	Milliliter
mM	Millimolar
mm	Millimeter
MNC	Mononuclear Cells
MO	Monocyte
mOSCAR	Mouse OSCAR
mRNA	Messenger RNA
MW	Molecular Weight
MΦ	Macrophage
NaCl	Sodium Chloride
NEMO	NF-κb Essential Modulator
NFAT	Nuclear Factor of Activated T Cells
ng	Nanogram
NK	Natural Killer
NLS	Nuclear Localization Signal
nm	Nanometer
OCIF	Osteoclastogenesis Inhibitory Factor
OCs	Osteoclasts
OD	Optical Density
ODF	OC Differentiation Factor
Oligo-nt	Oligo-Nucleotide
OPG	Osteoprotegerin
OPGL	OPG Ligand
OSCAR	Osteoclast-Associated Receptor
PAGE	Polyacrylamide Gel Electrophoresis
Pam3Cys	Synthetic Palmitoylated Mimic of Bacterial Lipopeptides
PBL	Peripheral Blood Leukocytes
PBS	Phosphate-Buffered Saline
PCR	Polymerase Chain Reaction
PFAAP5	Phosphonoformate Immuno-Associated Protein 5
pg	Picogram
pH	Pondus Hydrogenii (Latin) or Potential of Hydrogen
PHA	Phytohemagglutinin
PIAS3	Protein inhibitor of activated STAT3
PKC	Protein Kinase C
PMA	Phorbol Myristate Acetate
PWM	Pokeweed Mitogen
R-848	Imidazoquinoline Resiquimod

RACE	Rapid Amplification of cDNA Ends
RANKL	Receptor Activator For NF-κB Ligand
RBM	Rat Bone Marrow
RDA	Representational Difference Analysis
RHD	Rel-Homology Domain
RIPA	Radioimmunoprecipitation
RNA	Ribonucleic Acid
rpm	Revolutions Per Minute
RPMI	Roswell Park Memorial Institute
SD	Synthetic Defined Media
SDS	Sodium Dodecyl Sulfate
SF	Serum-Free or Superfamily
ss	Single Strand
TBS	Tris-Buffered Saline
TE	Tris EDTA
TIR	Toll/IL-1R
TLR	Toll-like receptor
TM	Trans-Membrane
TNF-α	Tumor Necrosis Factor Alpha
TPA	Tetradecanoylphorbol Acetate
TRAF-6	TNF Receptor-Associated Factor-6
Trp	Tryptophan
URP2	UNC-112 Related Protein 2
x *g*	*G* Force
X-Gal	5-Bromo-4-Chloro-3-Indolyl-β-D-Galactopyranoside
α-MEM	Alpha Modification of Eagle's Medium
κB	Kappa B
µg	Microgram
µl	Microliter

INTRODUCTION

Inflammation is "a local response to cellular injury that is marked by capillary dilatation, leukocytic infiltration, redness, heat, and pain and that serves as a mechanism initiating the elimination of noxious agents and of damaged tissue" (Merriam-Webster's Online Dictionary http://www.m-w.com/dictionary). The process of inflammation is designed to dilute, destroy, or otherwise inactivate the agent that caused the injury with the ultimate goal to restore damaged or infected tissue to its original state. Inflammation itself and the causative agent(s) can result in tissue destruction and bone loss with a wide range of debilitating effects. Examples are chronic periodontitis, rheumatoid arthritis and endotoxic or septic shock. Although such examples are different in their outcomes, they share common cells and signaling pathways and may also be regulated by common molecules.

Cells of the monocyte (MO)/macrophage (MΦ) lineage play a crucial role in the initiation and maintenance of inflammation. Historically, they were called the mononuclear phagocyte system (MPS) that was defined as a family of cells arising from bone marrow progenitors, circulating as MOs and entering the tissues where they form the resident MΦ population.[1] These cells differentiate from pluripotent stem cells in bone marrow and can differentiate into MΦs, osteoclasts (OCs) or dendritic cells (DCs).[2,3] In inflammatory processes, circulating MOs are quickly become recruited and activated into MΦs by bacterial products like lipopolysaccharides (LPS) and/or cytokines. It has been established that MΦ-colony-stimulating factor (M-CSF) is mainly a MΦ inducing cytokine, hence the name, but it

induces OC differentiation as well.[4,5] MΦs participate in the inflammatory and immune response by secreting pro- and anti-inflammatory mediators and by acting as phagocytes and antigen presenting cells. The balance between the two groups of cytokines is crucial for the modulation of inflammatory response. The signaling pathways for differentiation, maturation and activation of MΦs are important and have been used for drug development.[6-8]

OCs are multi-nucleated cells responsible for bone resorption and originate from the MO/MΦ lineage.[9,10] The highly regulated balance between bone resorption by OCs and bone formation by osteoblasts determines and maintains the skeletal mass under physiologic conditions. The disturbance of this balance can lead to severe pathologic conditions like osteoporosis and inflammatory diseases that involve bone like periodontitis or osteoarthritis. In addition to the balance between these two types of cells, there is an interesting osteoblastic role in the differentiation of OCs. Osteoblasts express two molecules essential and sufficient for OC differentiation; M-CSF [10,11] and TNF-related activation-induced cytokine (TRANCE) that is also known as receptor activator of NF-κB (RANK) ligand (RANKL), osteoprotegerin (OPG) ligand (OPGL), or OC differentiation factor (ODF).[10,12] M-CSF is expressed and secreted and it binds to its M-CSF receptor (CSF-1R or c-Fms) expressed on OC precursors, while RANKL is expressed on the surface of osteoblasts, stromal cells and T-lymphocytes, which requires physical cell-cell interaction to bind to its receptor RANK.[10] OPG is a secreted "decoy" receptor that can bind RANKL and inhibit or potentially regulate osteoclastogenesis, hence the other name osteoclastogenesis inhibitory factor (OCIF).[13] *In vitro* osteoclastogenesis has been successful when MΦs are cultured with M-CSF and RANKL.[9,10,12,14] It is interesting that IL-3 has been shown to block OC formation during the M-CSF/RANKL induction diverting the cells to MΦ differentiation.[15]

LPS which is found in the wall of gram-negative bacteria is a very potent activator for both the immune system and the skeletal system and their cells. It is pathologically found in the active sites of periodontal lesions.[16] In pathologic situations, over-stimulation by bacterial LPS and the enhanced survival of MΦs could lead to excessive release of cytokines, resulting in uncontrolled systemic inflammation and septic shock.[17-19] LPS acts by binding to the LPS receptor complex that is composed of 3 proteins-CD14, Toll-like receptor 4 (TLR-4), and myeloid differentiation protein-2 (MD-2).[8] CD14 is expressed on MOs and MΦs and is critical for LPS signaling.[20] LPS binds to a plasma protein called LPS-binding protein (LBP), which transfers LPS to CD14. CD14 has no cytoplasmic domain so it presents LPS to TLR-4/MD-2.[21] TLRs and IL-1 receptors form the Toll/IL-1R (TIR) super-family.[22] This family shares a common signaling pathway using TNF receptor-associated factor-6 (TRAF-6) and activating NF-κB transcription factor. LPS' effect on MO/MΦ cell line has been extensively studied, yet much more needs to be resolved. It has been shown that LPS-stimulated MΦ has a very large change in the gene expression profile to the extent that very few genes do not change their level of expression.[23] It has also been shown that TLR-4-LPS pathway induces pro-inflammatory cytokines in the precursors of OCs but not OCs themselves,[24] which supports that the stimulation of TLRs favors immune responses and inhibits osteoclastogenesis.[25] On the other hand, LPS has been shown to stimulate survival and fusion of pre-OCs.[11] Furthermore, LPS inhibits osteoclastogenesis by down-regulating M-CSF and RANK receptors on pre-OCs, however, it stimulates TNF-α-dependent osteoclastogenesis in RANKL-pretreated cells.[26] As for DCs, LPS activates existing DCs but inhibits the generation of new DCs.[27] An interesting feature of LPS is that pre-exposure to

low dose of it desensitizes the cells to a second challenge, known as LPS hypo-responsiveness or tolerance.[28,29]

The balance between pro- and anti-inflammatory cytokines, between the activation and the inhibition of cells and between the differentiations of different cell populations is crucial for the modulation of inflammatory response, bone physiology and the pathophysiology of the whole body. This balance is controlled by cell surface receptors. The expression of a receptor and its binding to its ligand initiates the signaling pathway(s) needed for a certain biological process. These receptors, ligands and their signaling pathways for differentiation, maturation and activation of cells are highly regulated and not fully elucidated.

A large group of gene families of these receptors are mapped on chromosome 19q13.42, forming the Leukocyte Receptor Cluster (LRC) [30] which is part of the Immunoglobulin Super-family (Ig-SF). These genes and gene families within this cluster share common structural and functional properties. They include killer cell inhibitory receptors (KIR),[31] killer cell activatory receptors (KAR),[32] leukocyte Ig-like receptors (LIR) [33,34] also known as Ig-like transcripts (ILT),[35,36] monocyte/macrophage (myeloid) inhibitory receptors (MIR),[37] HM and HL clones,[38] CD85 [39] or Leukocyte Ig-like receptors (activating LILRA or inhibiting LILRB) according to the Human Genome Organization (HUGO) Gene Nomenclature Committee HGNC (http://www.gene.ucl.ac.uk/nomenclature/genefamily/lilr.php); human hematopoietic Fc receptor for IgA (FcαR),[40] and leukocyte-associated Ig-like receptors (LAIR).[41] The two largest families are the KIRs/KARs and the LILRs. They both can be classified into three functional categories: inhibitory, activating and soluble secreted receptors. Members of the

inhibitory receptors have 2 or 3 extra-cellular Ig-like domains in case of KIRs and 2 or 4 in case of LILRBs. They have a long cytoplasmic tail that has one or more immunoreceptor tyrosine-based inhibitory motif (ITIM). Members of the activating receptors have short cytoplasmic tail that has no ITIMs. They have a charged AA residue (arginine in the case of LILRAs) in the trans-membrane (TM) domain and they activate the cells by the association of this residue with an immunoreceptor tyrosine-based activation motif (ITAM)-bearing adaptor protein (like FcRγ, DAP12 and CD3ζ). The soluble secreted receptors retain the extra-cellular Ig-like domains and the signal peptide but lack the TM domain. The expression distribution of LRC genes is variable. While KIRs/KARs are expressed only in natural killer (NK) cells and T cells, LILRs are expressed in lymphoid and myelomonocytic cells including T, B and NK cells, monocytes, macrophages and dendritic cells.[34,42] LAIRs are even broader in their expression range.[41]

We have isolated a novel gene, 3D10, which is an alternative spliced isoform of the newly discovered Osteoclast-Associated Receptor (OSCAR).[43] OSCAR is one of the most recently identified members of the LRC genes. It was discovered in mouse and thought to be OC-specific gene. Human OSCAR (hOSCAR) shows structural and functional similarities to the LILRAs. It has two extra-cellular Ig-like domains, arginine residue in the TM domain and a short cytoplasmic tail. It has been shown to associate with FcRγ and activates dendritic cells.[44] This shows that hOSCAR is a classical activating leukocyte receptor. hOSCAR expression has been reported in neutrophils, monocytes, macrophages and dendritic cells.[44] Its expression in human tissues has not been fully explored and there have been no identified stimuli to modulate its expression. The fact that its ligand has not been identified either, adds to the complication of its investigation. Lately, hOSCAR has been studied extensively and

new findings show the importance of this receptor in modulating the innate and the adaptive immunity in addition to its involvement in bone biology.

This research investigates a novel soluble group of hOSCAR focusing on 3D10 as a representative of this group. We present some expression data of this group comparing it to the membrane-bound group and show some novel findings related to the modulation of the expression of both groups. We also present some potential binding partners that might include OSCAR ligand which has been considered the most important finding to study OSCAR function by many authors. These partners might also include important modulators to the osteo-immune biology. Findings from this research will definitely contribute to the understanding of human biology and the future development of therapeutic modalities for diseases

Chapter 1. 3D10 is a New Isoform of the Osteoclast-Associated Receptor

Background

Our laboratory has been studying bone biology, wound healing and the extra-cellular matrix biology. This project started when we were searching for genes that are differentially expressed during bone remodeling in neonatal mice. At this stage of development, tissues and cells behave very similar to the wound healing process.[45] During these processes some genes are up-regulated and differentially expressed. To identify some of these genes, the Representational Difference Analysis (RDA) method has been proposed. RDA has been originally designed to analyze the differences between two complex genomes and has been used to isolate probes to viral genomes present as single copies in human DNA.[46] RDA can also be used to analyze differences between two cDNA samples in the same way.

Since we were searching for mouse bone-specific genes, bone tissue should be used to synthesize the "Tester" cDNA. The "Driver" cDNA should be synthesized from tissues that share the same genes except bone-specific genes like skin and tail. We performed this method and isolated two novel genes one of which was 3D10.

Materials and Methods

Representational Difference Analysis

Twenty 7-day-old C57BL/6J mice (Black 6) of unknown sex were sacrificed by quick decapitation. Calvaria (target tissue or tester), skin, and 1 cm tail samples (control/driver

tissues) were dissected out and kept in ice-cold phosphate-buffered saline (PBS) buffer treated with diethyl pyrocarbonate (DEPC). Tissues were immediately homogenized in guanidine thiocyanate for total RNA isolation in cesium chloride (CsCl)-gradient method.[47] The isolated RNA was treated with RNase-free DNase and then checked for quality using formaldehyde-agarose gels. Magnetight™ Oligo(dT) Particles (Novagen, EMD Biosciences, Inc, Darmstadt, Germany) were used to isolate messenger RNA (mRNA) from 200 μg of total RNA from each tissue type. RDA was completed according to a published protocol.[48] Briefly, single stranded (ss) DNA was obtained using Superscript II Reverse Transcriptase (Invitrogen) and mRNA as template. Double stranded (ds) cDNA was synthesized by *E. coli* DNA polymerase, quality assessed in agarose gels and cut with the restriction enzyme DpnII. Cut fragments were polymerase chain reaction (PCR)-amplified giving the Representations for each cDNA type. Approximately 1.5 μg of each cDNA type was ligated to the R-Bgl-12/24 adapter in a PCR machine using T4 DNA ligase and oligonucleotides (oligo-nt). The amplified products were verified on agarose gel, phenol extracted-ethanol precipitated and re-suspended in buffer TE. DpnII digestion removed the R-adapters and then Qiaex resin was used to gel-purify the Representations. A new set of J-Bgl-12/24 adapters were ligated to the tester cDNA as described for R-adapters. The driver tissue cDNA was pooled with no adapters ligated and 40 μg of it was mixed with 0.4 μg of the tester. This mixture was phenol extracted-ethanol precipitated and thoroughly re-suspended in 4 μl of EEx3 buffer (30 mM EPPS, pH 8.0, 3 mM EDTA). Mineral oil was overlaid, DNA was denatured and the salt concentration was adjusted by adding 1 μl of 5 M NaCl. The sample was allowed to anneal/hybridize. The hybridized DNA was diluted, re-suspended in 400 μl of TE and 10-cycle-PCR amplified. All ssDNA was removed using mung bean nuclease in digestion

buffer. Final amplification was carried out by PCR for 18 cycles. The PCR product was phenol extracted, isopropanol precipitated and re-suspended at 0.5 μg/μl to give the First Difference Product (DP1).

The Second Difference Product (DP2) was generated using the N-Bgl-12/24 adapters and the same steps of DP1 except that in the second round of hybridization, 50 ng of tester (DP1) was mixed with 40 μg of driver. The procedure was repeated a third time using 100 pg of J-ligated DP2 to generate the "final" Third Difference Product (DP3), which was the result of 22 cycles of PCR amplifications. DP3 was digested with DpnII and cloned into the BamHI site of the vector pSPORT-2 (Invitrogen) and screened for recombinants by blue-white screening. Randomly picked white colonies were grown and plasmid DNA prepared using the Qiagen kit for minipreps (Qiagen, Inc.). Forty one colonies were sequenced and their cDNA was compared with entries in GenBank Sequence Database.

Northern Blotting

Total RNA was isolated from the calvaria, skin and tails of 7-day-old mouse pups as described previously. Twenty μg of total RNA from each tissue was run on formaldehyde agarose gels and blotted onto Nylon membranes. The complete protocol is described elsewhere.[49] The membranes were processed for Northern Blotting using ^{32}P-dCTP-labeled probe for 3D10. Ethidium bromide-stained gel was used for loading comparison.

3D10 cDNA Cloning

3D10 cDNA was sequenced and analyzed for homology. A newly described Osteoclast Associated Receptor (OSCAR) [43] and a human EST clone showed significant homology.

Because of the differences with OSCAR, we sequenced the human EST clone and identified a 282-amino acid (AA)-coding region. This sequence showed that 3D10 is an alternatively spliced variant of OSCAR gene with an un-spliced intron between the last two exons giving a larger transcript. This intron has a stop codon preventing the last exon from being translated. We cloned the coding region of human 3D10 plus the un-translated region from the last exon to the stop codon into the eukaryotic expression vector pcDNA3.1/His B (Invitrogen) which has an amino (N)-terminus Xpress epitope and a His-tag (Figure 1.1).

Anti-3D10 and Anti-mOSCAR Antibodies

Using the human 3D10-specific C-terminus polypeptide we synthesized a polyclonal antibody. The C-terminal 15 AA-polypeptide (QDSWDPAPPPSDPGV) was conjugated to keyhole limpet hemocyanin (KLH) and used to immunize rabbits. Pre-immune serum was prepared to be used as a negative control. This was made by Alpha Diagnostic Intl. Inc., San Antonio, TX. We received 6 bleeds from 2 rabbits. Aliquots were prepared and stored at -80°C. Anti-mOSCAR Ab (R&D Systems) was raised in goat against AA 19-228 of mOSCAR, which is approximately 70% homologous to the N-terminus sequence of hOSCAR.

3D10 mRNA Expression

Human BD™ MTC Multiple Tissue cDNA Panels (Human MTC Panel I, and Human Immune System MTC Panel of Clontech) were PCR-amplified using 3D10-specific primers. PCR products were hybridized with ^{32}P-dCTP-labeled probe for 3D10. GAPDH was used for loading control.

3D10 Protein Expression

A common cell line for MΦ and OC is the murine myeloid cell line RAW 264.7 (ATCC TIB-71). RAW 264.7 is MΦ-like, Abelson leukemia virus transformed cell line derived from BALB/c mice. RAW 264.7 cells were plated and incubated in Dulbecco's modified Eagle's medium (DMEM) with 10% fetal calf serum (FCS) to adhere for 24 hours (h). One μg/ml *E. coli* LPS (Sigma) was added in fresh medium and cell lysates were collected at 0 (no LPS), 2, 6, 12 h, 1, 2, 4 and 6 days in RIPA buffer. Equal amount of protein from each time-point was loaded in 4-12% SDS-Poly Acrylamide Gel Electrophoresis (PAGE) gels and transferred to 3 celluloid membranes for western blot using TNF-α and IL-1β antibodies (R&D Systems) and 3D10 rabbit anti-sera.

We also examined LPS effect in cultured bone marrow cells. Adult rats were sacrificed under CO_2 chambers, the long bones were dissected out from all adherent tissues carefully and the bone marrow was flushed with α-MEM. The marrow was homogenized, centrifuged and cultured in α-MEM/10% FCS for 24 h. Non-adherent cells were collected and cultured for the LPS experiment. LPS was added in fresh medium and 2 days later lysates were blotted using 3D10 anti-sera and goat anti-mOSCAR antibody.

Adult Black 6 mice were sacrificed under CO_2 chambers. Skin, lung and spleen samples were dissected out and kept in ice-cold PBS buffer containing 1X proteases inhibitor cocktail (Sigma). Tissues were homogenized and protein was extracted by centrifugation. Total protein was measured using BCA (bicinchoninic acid) Protein Assay (Pierce). Aliquots of equal loading were processed for western blot and blotted with anti-3D10 anti-sera.

Immunohistochemical staining of serial paraffin sections generously obtained from Dr. Dana Graves, Boston University, were processed and analyzed as follows. Slides were heated to 55-60ºC for 20 min to melt paraffin. Gradual re-hydration was done by immersing in xylene for 5 min twice followed by serial dilution of ethyl alcohol from 100% to dH_2O at 5 min intervals. Slides were immersed in boiled 1 mM EDTA (pH 8) for 1 min followed by dH_2O and then PBS for 5 min each. Endogenous peroxide was blocked by immersing the slides in 50% methyl alcohol and 1% H_2O_2 for 30 min. Non-specific antigens were blocked by 1:100 pre-immune serum in PBS for 30 min. Slides were stained then by either pre-immune serum or anti-3D10 anti-sera followed by the secondary antibody.

Transient transfection of RAW 264.7 cells was carried out using Superfect transfection reagent (Qiagen) according to the manufacturer's protocol. Cells were transfected with 3D10 eukaryotic expression vector pcDNA3.1/His B, lysed and blotted using 3D10 antibody.

Recombinant 3D10 Production

3D10 cDNA was cloned into the prokaryotic expression vector pET-15b (Novagen) which is inducible and has an N-terminus His tag. Plasmid was verified for its reading frame by sequencing, amplified and isolated from non-expression host NovaBlue. It was then transformed into expression host *E. coli* strain BL21(DE3). Single colonies from Luria Broth (LB)/ampicillin (amp) plates were tested for expression by inoculating the bacteria into 3 ml LB/amp media and incubated at 37°C and shaking at 250 rpm for 3 h followed by 1 mM IPTG induction for 1 h. Samples from cultures (before and after induction) were run in SDS-PAGE and initially verified by immuno-blotting in western blot using anti-3D10 anti-sera.

All other small scale cultures thereafter were tested by Coomassie blue staining looking for protein expression at the expected molecular weight. Positive cultures were scaled up. Cells were harvested by centrifugation at 4°C and 6500 x *g* for 15 min. Protein was isolated as either soluble or insoluble (in the inclusion bodies) by binding, washing and eluting buffers in His-Bind resin columns according to the manufacturer's instructions (Novagen pET System).

Results

mOSCAR is differentially expressed in developing bone

Out of the 41 clones we sequenced, two clones were novel at the time this was done (Table 1.1). The novel clone we named 3D10 (in mouse) was later registered as mOSCAR. We isolated a 240 bp-fragment near the 5' end of this transcript. We synthesized a ^{32}P-dCTP-labeled probe using the whole fragment. Northern blot confirmed that 3D10 is expressed in calvaria and not in skin or tail of neonatal mice (Figure 1.2). Several attempts were made unsuccessfully to isolate the full cDNA using Rapid Amplification of cDNA Ends (RACE). We found the human EST clone which was approximately 70% homologous to the isolated fragment and named it 3D10. All the following studies were made to characterize the human 3D10.

3D10 mRNA is widely expressed in human tissues

We found that the strongest expression among the examined tissues was from peripheral blood leukocytes (Figure 1.3). Weaker signals were also observed from lung, pancreas, kidney, spleen, liver, bone marrow and placenta. Another human 24-tissue cDNA panel

(OriGene) was used to compare the expression of soluble group with the membrane-bound group. This is discussed in chapter 4.

3D10 protein expression is observed in mouse tissues

Western blot of spleen, lung and skin using 3D10 rabbit anti-sera showed a single band with the expected molecular weight (MW) of ~ 32 kDa (Figure 1.4). Although skin showed negative expression to 3D10 during the RDA and the Northern blot, it was from 7-day-old pups while for western blot it was from adult mice. Furthermore, skin sample for western blot contained inflammatory cells and dendritic cells that have been found to express 3D10 and human OSCAR respectively.[50]

Immunohistochemical sections of various tissues showed positive 3D10 staining in OCs and inflammatory cells compared to the control rabbit IgG or normal goat serum (Figure 1.5).

Cloned 3D10 is over-expressed in RAW 264.7 cells

Transiently transfected RAW 264.7 cells showed a prominent band with the expected MW of 3D10 matching the band from non-transfected cells (Figure 1.6).

LPS-stimulated RAW 264.7 and RBM cells over-express 3D10

The expression of 3D10 in leukocytes and OCs guided us to study LPS effect on its expression *in vitro*. LPS-stimulated RAW 264.7 (Figure 1.7) expressed TNF-α and IL-1β with the first time-point post-LPS addition (2 h). While TNF-α and IL-1β had different peaks, they both gradually decreased when 3D10 expression started to gradually increase

from the baseline that did not change with LPS addition. The time-course of the experiment did not allow us to compare the peak of 3D10 expression with the other 2 pro-inflammatory cytokines. Nevertheless, there was an obvious inverse relationship between them.

RBM cells showed similar baseline expression of 3D10 and over-expression post-LPS stimulation (Figure 1.8). Anti-mOSCAR Ab did not detect any expression.

3D10 cloned and expressed using prokaryotic expression system could not be purified

Initial induction test for 3D10 expression was positive as western blot showed (Figure 1.9). The expressed protein was found in the pellet as inclusion bodies. Several protocols were used to solubilize it and purify it unsuccessfully. Another host strain (BL21(DE3) pLysS) was used, slow expression at 30°C, addition of 1% glucose to repress lac promoter, different buffers (like phosphate or Tris buffers), denaturation by 6 M urea or guanidine HCl, adding reagents like DTT or Triton X, and extreme pH (4.6 and 9.1) were all unsuccessful. We tried to lyophilize the pellet and re-dissolve it but the protein remained in the pellet.

Discussion

We have shown that mOSCAR is differentially expressed during bone remodeling in neonatal mice. OSCAR has been shown to be important in OC differentiation.[43,51] The balance between OC and osteoblast function is very important in the development and wound healing. In addition to this, we have also shown that OSCAR is expressed in other tissues and cells and may play important role in modulating the immune response. More data and findings will be shown in the following chapters of this project.

3D10 coding transcript is currently registered at GenBank as human OSCAR isoform OSCAR-S1 by Kim et al. We isolated mouse OSCAR fragment and obtained a human EST clone that was approximately 70% homologous to the isolated fragment and different from mouse OSCAR at the C-terminus. When mOSCAR and hOSCAR genes were identified with their supporting transcripts we compared the sequences and realized that there is no evidence that supports the existence of the soluble group in mouse. The Ab we synthesized and used recognized a sharp strong band at the expected molecular weight of 3D10 in mouse tissues and the murine cell-line RAW 264.7. This band is increased in intensity with LPS stimulation in both mouse and rat tissues. Immunohistochemistry slides showed positive staining of multi-nucleated giant cells located at bone margins that looked characteristic of OCs. Inflammatory cells also showed positive staining compared to the pre-immune serum control. Finally, there was no homologous match or close to the epitope we used to synthesize anti-3D10 Ab when we searched in mouse protein database using Blast. These findings and observations support that anti-3D10 Ab could be binding to a mouse homolog of 3D10 that has not been identified and isolated. The possibility that anti-3D10 Ab cross-reacts to another molecule sharing the same antigenicity and molecular weight with 3D10 is supported with the mouse genomic structure of OSCAR gene and the negative results observed when anti-mOSCAR Ab was used. This Ab was raised to an epitope that is approximately 70% homologous to hOSCAR. Nevertheless, many antibodies may fail to bind to proteins carrying the epitope for unknown reason. The final answer will be determined when the band recognized by anti-3D10 Ab is precipitated and sequenced. This is one of the future directions of 3D10 investigation.

Recombinant 3D10 could not be purified from a prokaryotic expression system. The expressed protein is different from the native eukaryotic one in at least two areas. It lacks any post-translational modification and it has the N-terminus addition of His tag and linker. Human OSCAR has been shown to be N-glycosylated.[50] It has 3 potential sites that are present in 3D10 sequence. N-glycosylation is important in protein folding and stability and could have contributed to the unsuccessful 3D10 purification. Lower level of expression could be attained and purified from eukaryotic expression system or from transfected cells, provided that the protein is not toxic to the cells or unstable for other reasons.

Although we were interested in the extra-cellular matrix biology, the progress of this project has shown and proven that biological systems are complex and inter-related. OSCAR has been shown to be important in both the immune system and the skeletal system. The field of the cross-talk between skeletal system and immune system "Osteoimmunology"[52] has been growing lately. Both systems have common regulatory molecules (e.g. RANKL[53], IFN-γ[54], IFN-β[55] and other cytokines), and cells of both systems form in the bone marrow. Bone regulation by immune inflammatory processes and the "inflammatory bone loss" are very well recognized but the complete picture is not completely understood. Understanding the biological mechanisms between the two systems has a definite positive impact on our health.

In conclusion, 3D10 is a new isoform of hOSCAR. It is expressed in wide variety of tissues and cells. It might be expressed in mouse and is up-regulated with LPS stimulation.

The following chapters will focus on the role of 3D10 in modulating inflammation by inhibiting NF-κB transcription factor activity, searching for 3D10 binding partners and

characterizing the soluble group of hOSCAR compared to the membrane-bound group regarding the expression and distribution pattern.

Tables

Table 1.1. Representational Difference Analysis of 7-day-old mouse calvaria (tester) and skin/tail (driver) after 22-cycle PCR amplification DP3.

Number of Clones	Sequence Homology to GenBank entries	Confirmation by Northern Blotting
25	Mouse Osteocalcin	Yes
2	Mouse Acid Phosphatase	Yes
2	Mouse Creatine Kinase	Yes
6	Rat Myosin Heavy Chain	No
4	Unknown Protein mRNA (mouse)	No
1	Novel Clone 3D10	Yes
1	Novel Clone 4G8	Yes

Figures

Figure 1.1. Cloned 3D10 into pcDNA3.1/His B.

Full coding region of 3D10 cDNA (3D10 CDS) plus the un-translated region of the last exon to the stop codon of membrane-bound hOSCAR was cloned into the vector pcDNA3.1/His B (Cloned fragment). KpnI and BamHI restriction sites were used at the 5' and 3' ends of the insert respectively. An additional "c" nucleotide was added after the KpnI site to make the insert in-frame. The vector has an N-terminus 6-histidine (6xHis) tag and an Xpress epitope. EK: enterokinase recognition site, BGH pA: Bovine Growth Hormone polyadenylation region, Neo®: Neomycin resistance gene, Amp®: Ampicillin resistance gene.

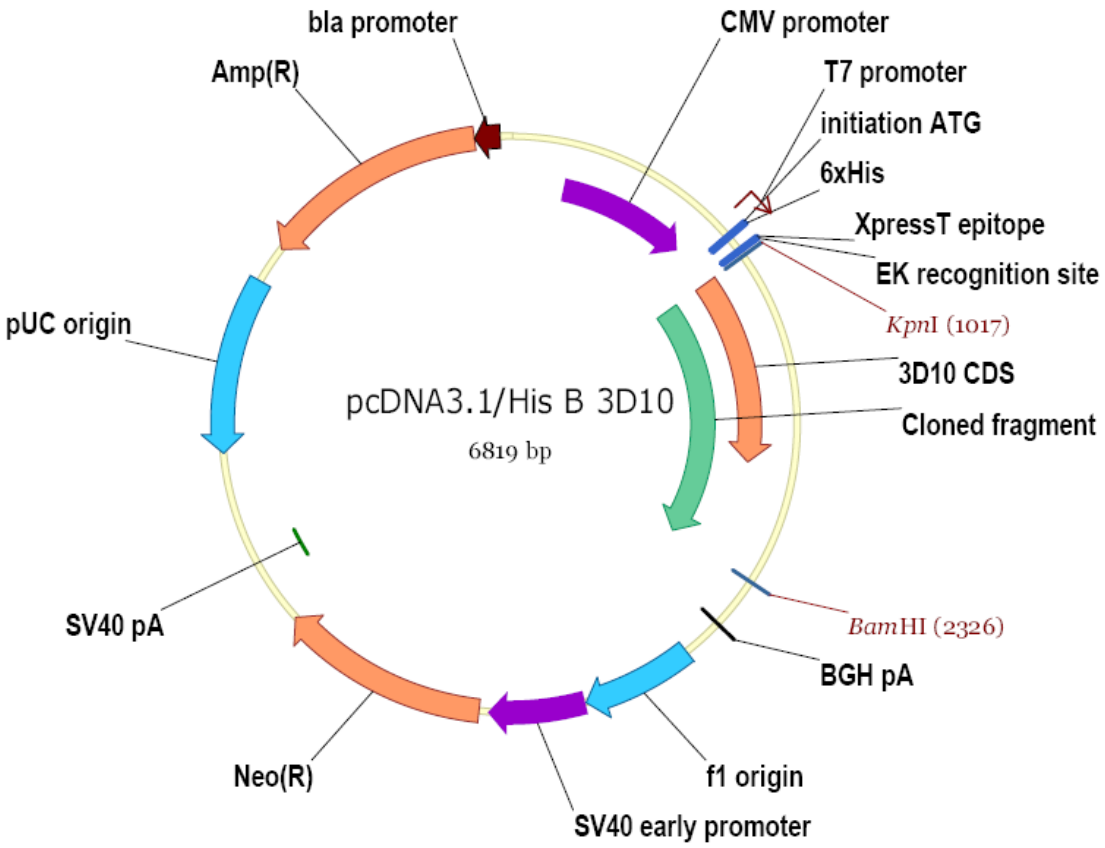

Figure 1.2. Northern Blot Confirming RDA results.

20 μg total RNA from calvaria (C), skin (S) and tail (T) of 7-day-old mouse pups was run on formaldehyde agarose gels and blotted onto Nylon membranes. The membranes were processed for Northern Blotting using ^{32}P-dCTP-labeled probes for 3D10 (Left). The blot shows that 3D10 is expressed in calvaria and not in skin or tail. Ethidium bromide-stained gel shows loading of total RNA (Right). The positions of 28S and 18S ribosomal RNA are indicated.

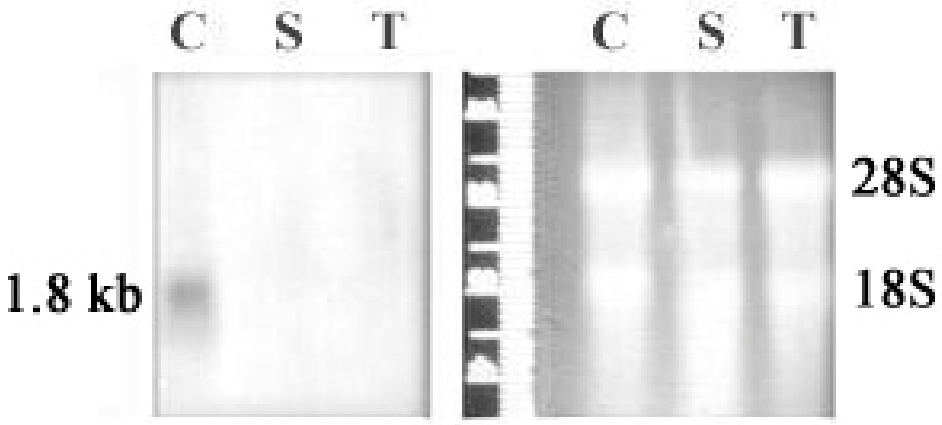

Figure 1.3. PCR amplification of 3D10 mRNA expressed in human multiple-tissue cDNA panel.

3D10 cDNA was amplified from Human BD™ MTC Multiple Tissue cDNA Panels (Human MTC Panel I, and Human Immune System MTC Panel of Clontech) using 3D10-specific primers in PCR and the products were hybridized with ^{32}P-dCTP-labeled probe for 3D10. 3D10 is heavily expressed in peripheral blood leukocytes (PBL). Weaker signals were also

observed from lung, pancreas, kidney, spleen, liver, bone marrow and placenta. GAPDH probing shows the relative loading differences. The large difference in loading is due to the mixture of two panels without specific order.

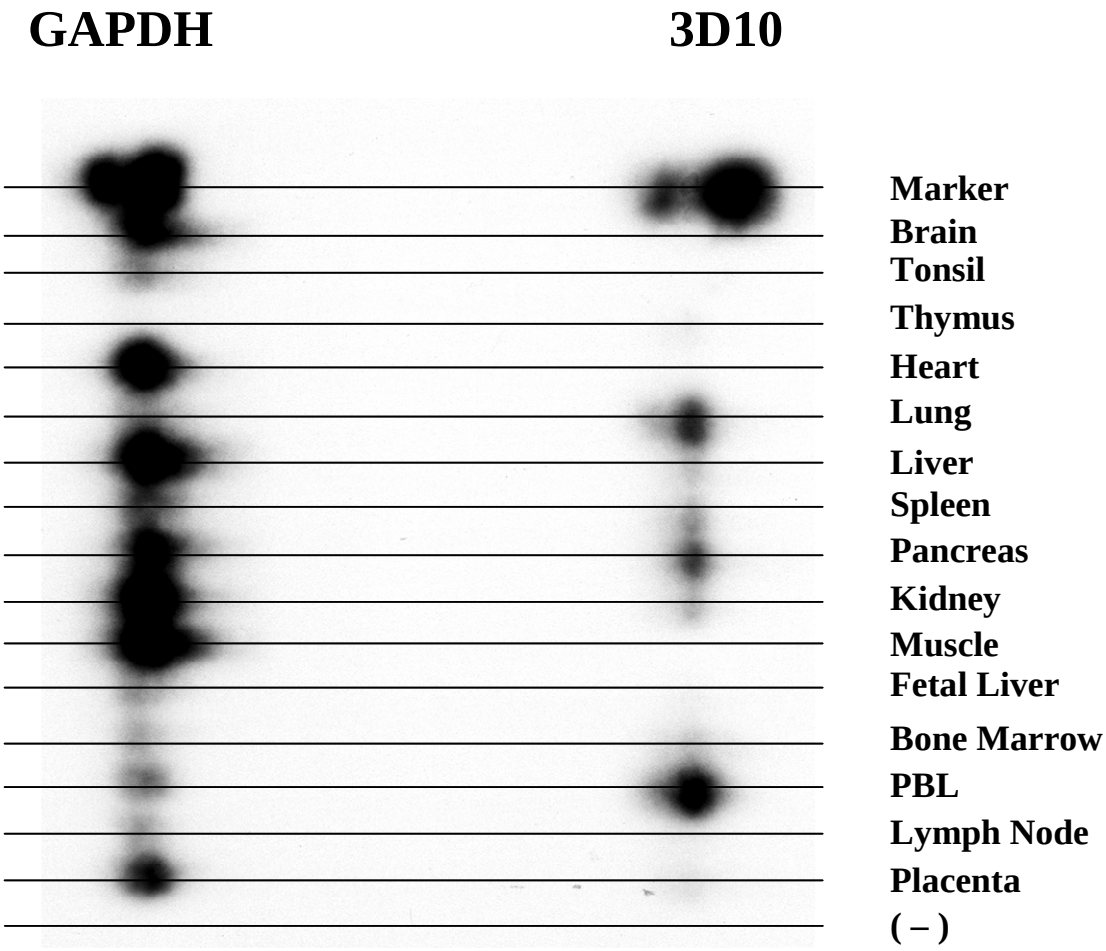

Figure 1.4. Western blot of adult mouse tissue extracts using 3D10 antibody.

Lysates from adult mouse tissue extracts were processed for western blot as described and blotted using 3D10 antibody. 3D10 is heavily expressed in skin. Weaker signals were also

observed from lung and spleen. 3D10 expression in the skin might represent the inflammatory cells and/or the skin DCs as has been shown for human OSCAR.

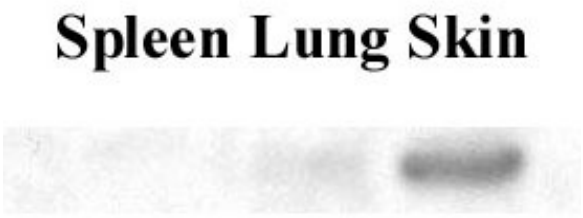

Figure 1.5. 3D10 is widely expressed by multi-nucleated giant cells, leukocytes and other cells in bone and gingiva of mice.

Immunohistochemical analyses of serial paraffin sections from mouse stained with either anti-3D10 Ab (1) or the pre-immune serum (2). (A) The inter-dental part of the periodontium of adult mouse showing the inflammatory cells in the lamina propria with positive 3D10 staining. Other cells in the gingival epithelium are also positive. (B) LPS-induced inflammation in mouse calvaria with subcutaneous injection (sections were generously obtained from Dr. Dana Graves, Boston University). OCs and inflammatory cells show positive 3D10 staining.

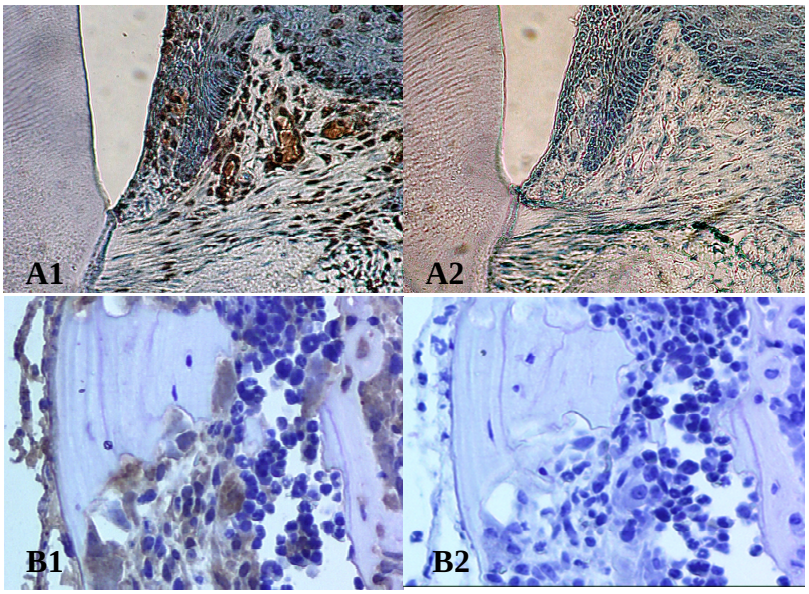

Figure 1.6. Western blot of transiently-transfected RAW 264.7 cells with 3D10.

RAW 264.7 cells were plated and transiently-transfected (TT) with pcDNA3.1/His B-3D10 using Superfect transfection reagent according to the manufacturer's protocol. Cells were lysed and blotted using 3D10 antibody. Transfected cells show a prominent band with the expected MW of cloned 3D10 compared to the band from non-transfected control (C) cells.

Figure 1.7. RAW 264.7 cells express 3D10 and it is up-regulated with LPS stimulation at the time IL-1β and TNF-α are down-regulated.

RAW 264.7 cells were plated at approximately 70% confluence in 100 mm dishes and stimulated with 10 μg/ml *E. coli* LPS 24 h post-plating. Cell lysate was processed for western blot at the indicated time points and blotted using anti-3D10, anti-mouse IL-1β or anti-mouse TNF-α antibodies. 3D10 maintains a stable baseline expression and is up-regulated with the decreased expression of IL-1β and TNF-α, post-LPS stimulation. mTNF-α is the membrane-bound form.

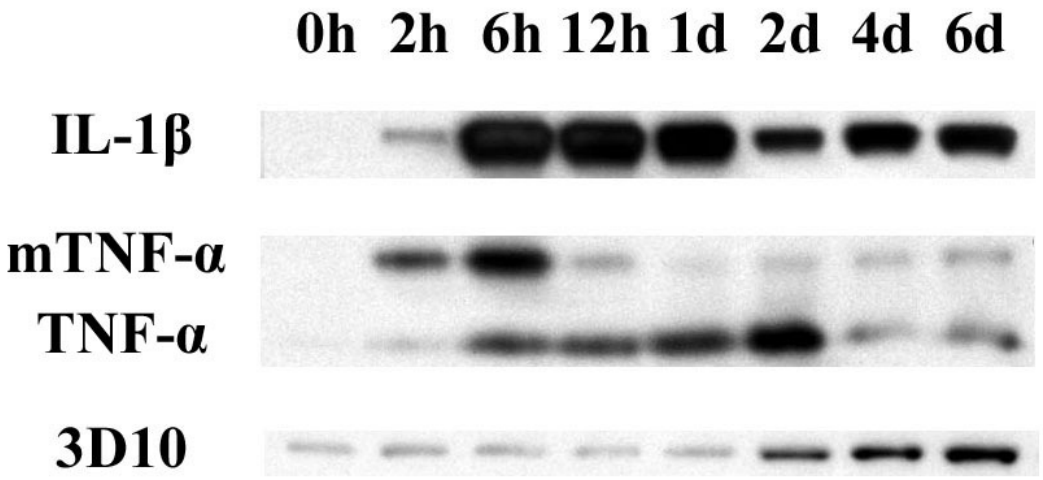

Figure 1.8. 3D10 is expressed by rat bone marrow (RBM) cells and is up-regulated by LPS stimulation.

Cultured rat bone marrow cells (RBM) were isolated and plated as described. LPS was added in fresh medium and 2 days later lysates were blotted using 3D10 anti-sera and goat anti mOSCAR antibody. 3D10 Ab recognized a baseline expression that was induced by LPS. Anti-mOSCAR Ab did not detect any band before or after LPS stimulation.

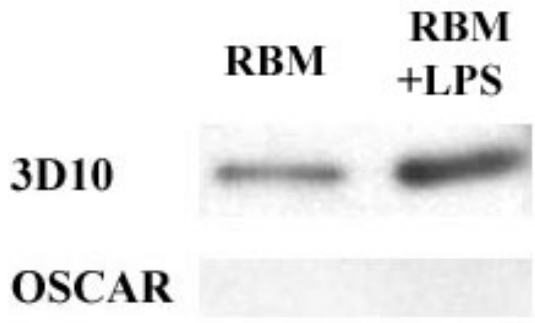

Figure 1.9. Western blot of bacterial expressed 3D10.

3D10 full cDNA was cloned into the prokaryotic expression vector pET-15b and transfected into *E. coli* cells as described. After 3 h of small scale cultures, before and after induction (BI and AI) aliquots (7 μl) and samples from the supernatant (SN) and the pellet (P) of the large scale culture were run in SDS-PAGE and blotted in western blot using anti-3D10 anti-sera. 3D10 protein band is shown clearly in the sample from culture after IPTG induction and it is shown as a negative band in the pellet due to the high concentration.

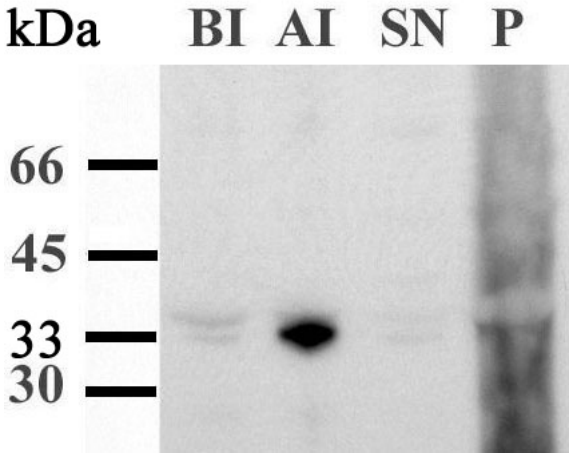

Chapter 2. 3D10 Inhibits NF-κB

Background

NF-κB represents a common and important regulatory transcription factor and signaling pathway for many pro-inflammatory cytokines including IL-1β and TNF-α.[56,57] NF-κB is a transcription factor family consists of 5 members: NF-κB1 (p50 or its precursor p105), NF-κB2 (p52 or its precursor p100), NF-κB3 (p65 or RelA), Rel (c-Rel) and RelB.[6,56] The active NF-κB is a homo- or hetero-dimer that forms through a conserved Rel-homology domain (RHD), which also serves as DNA-binding and principal regulatory domain.[6,56] The precursors p105 (p50) and p100 (p52) have their RHD fused to an auto-inhibitory Ankyrin repeats (ANK) common for all NF-κB inhibitory proteins (IκBs). IκBs bind to NF-κB units and mask the nuclear localization signal (NLS) - present on the RHD - trapping NF-κB in the cytoplasm.[56] Activation of NF-κB pathway by many stimuli (e.g. LPS) results in the proteasome degradation of IκBs mediated by phosphorylation and ubiqitination, and the nuclear translocation of NF-κB dimer.[6,56] The most common NF-κB (classical) is NF-κB1/NF-κB3 (p50/p65). Two protein complexes are essential for NF-κB release: the IκB-kinase (IKK) and the $E3^{I\kappa B}$ ubiqitin ligase complexes.[6] The IKK complex is composed of three subunits: the catalytic subunits IKK1 (IKK-α) and IKK2 (IKK-β), and the regulatory subunit NF-κB essential modulator (NEMO) (IKK-γ).[6,56] NEMO is required for IKK activity and p50/p65 activation but not the p52/RelB (alternative pathway). Classical NF-κB cannot be activated without IKK2 but IKK1 is required for RANK pathway.[6] NF-κB is an important

transcription factor in inflammation and immune response.[7,58] Factors that regulate NF-κB transcription and activity seem to be very important for therapeutic strategies.

Although NF-κB is not the only regulatory pathway for TNF-α and IL-1β, it is common to both cytokines and has very broad and diverse functions. Most of the studies focus on the early stages of LPS-induced cytokines production and kinetics. Reviewing that in summary, it has been observed that all NF-κB-dependent cytokines are produced very early post-LPS stimulation. They peak between 6 hours to 2 days. This peak is usually followed by a steady state and then declines to the basal level with the loss of inflammatory signs. Examples to this are TNF-α[59,60], IL-1β[60], IL-6[60] and iNOS.[61] Similar findings have been observed with non-NF-κB-dependent cytokines like IL-10[60] and IL-18 which is similar to IL-1β but with longer steady state.[62]

3D10 up-regulation was observed late during LPS-induced inflammation. This could be related to later stages of inflammation like cell migration, phagocytosis or LPS-tolerance, especially when we know that the last two are associated with NF-κB inhibition.[63-65]

We also investigated the effect of two nuclear proteins that were found to bind to 3D10 in the yeast-two-hybrid analysis. The first one is phosphonoformate immuno-associated protein 5 (PFAAP5) and the second is Human Leukocyte Antigens-B (HLA-B)-associated transcript 3 (BAT3). Nuclear proteins could modulate transcription factors like YAP (Yes-associated protein of 65 kDa)[66] and could act as chaperone pulling 3D10 into the nucleus. BAT3 is an apoptotic regulator.[67] NF-κB has been shown to regulate apoptosis.[68-71]

Since hOSCAR has been reported to enhance the pro-inflammatory cytokine production, we attempted to establish over-expressing stably transfected cells to investigate 3D10 as a possible antagonist to hOSCAR.

Materials and Methods

NF-κB Inhibition

We used the reporter plasmid 3X-κB-luc, which has 3 copies of the NF-κB binding site from the murine major histocompatibility complex (MHC) class I promoter upstream of the luciferase gene (a generous gift from Dr. Albert S. Baldwin, Lineberger Comprehensive Cancer Center, UNC-CH). Human embryonic kidney cells (HEK 293T) [72] were plated in 12-well plate at a density of 7.5×10^4 and allowed to adhere for 24 h. The approximately 70-80% confluent cells were transfected using Effectene transfection reagent (Qiagen) with 3X-κB-luc with or without the following plasmids: p65 (positive control), 3D10 in pcDNA3.1/His, or IκB-α super-repressor (negative control). As control for transfection efficiency, β-Gal construct was used for all wells. Total DNA was maintained by adding the appropriate blank vector if needed. 48 h post-transfection, cell lysates were collected and processed for luciferase and β-Gal activities (Promega) and read in a luminometer and plate reader respectively. The experiment was performed in triplicates. The averages were normalized and compared using Student's *t*-test. This experiment was repeated with different doses of 3D10 plasmid and also with some of its binding partners (PFAAP5 and URP2). Positive control p65 was replaced in some experiments with human recombinant TNF-α. LPS could not be used as positive control because HEK 293T cells do not express its receptor.

Cell Viability

An initial screening to the effect of 3D10 on cell viability was performed using CellTiter 96 AQueous One Solution Cell Proliferation Assay (Promega). HEK 293T cells were seeded in duplicate 96-well plates at 3 x 10^4 cells/well in 100 µl culture media. Cells were transfected with 3D10, PFAAP5 and BAT3 plasmids at different concentrations using Effectene rapid transfection protocol (Qiagen). 24 h post-transfection, cells in one plate were stimulated with 30 ng/ml TNF-α in fresh media to induce apoptosis, and the other plate was processed for reading as follows: 20 µl of CellTiter reagent was added to each well and the plate was incubated at 37°C and 5% CO_2 for 1 h. Soluble formazan produced by viable cellular reduction was measured by recording the absorbance at 490 nm using a 96-well plate reader. 24 h post-stimulation, the other plate was processed and read similarly. All wells were in triplicates and averages were compared.

Stably Transfected Cell-lines

To overcome the stress produced by transient transfection and to study the effect of 3D10 on cell differentiation, activation and survival, we generated stably transfected cell-lines. HEK 293T and RAW 264.7 cell-lines were plated and transfected as previously mentioned, with each of the following plasmids: 3D10, pcDNA3.1/His empty vector and OSCAR4 in pFLAG-CMV-4. Culture medium was replaced by a selection medium containing 1 g/ml G418 (Gibco). Cells were allowed to grow for 2-3 weeks in selection medium and fed every 3 days. Positive adherent colonies were collected and re-plated as needed in low density to allow true selection. Dead cells were removed regularly by washing and media replacement. Stably transfected cells were frozen and stored at -80°C.

Results

Initially, 3D10 showed significant inhibition to NF-κB activity (50% ± 4.8) compared to the super-repressor IκB-α (88% ± 0.3). 3D10 also showed a dose-response effect with 3 different concentrations of the DNA 0.1, 0.2 and 0.4 μg. Data represents the mean of triplicates ± standard deviation (Figure 2.1). Comparisons were statistically significant when $p < 0.05$. When compared to PFAAP5 (Figure 2.2) and URP2 (Figure 2.3), the former showed similar results to 3D10 while the latter needed higher plasmid concentration to achieve similar effect. When TNF-α was used as a positive control, it failed to activate NF-κB and 3D10 showed equivalent inhibition in both conditions (Figure 2.4). The experiment was modified to allow cells to rest after the transient transfection but during this experiment 3D10 showed no significant inhibition compared to the empty vector (Figure 2.5). We also investigated the effect of double transfection of 3D10 and PFAAP5 and this showed an additive effect (Figure 2.6).

Neither 3D10 nor PFAAP5 showed any significant effect on cell viability compared to the empty vector control. The same was observed when cells were stimulated to induce apoptosis (Figure 2.7).

Discussion

We presented here that 3D10 inhibited NF-κB baseline activation induced by the transient transfection stress by 30-50%. PFAAP5 showed the same level of inhibition and they both showed an additive effect. TNF-α-dependent activation could not be inhibited by 3D10 expression. NF-κB could be activated by many stimuli including TNF-α, IL-1, phorbol ester,

okadaic acid, H_2O_2, ceramide, endotoxin, and γ-radiation.[73] We only investigated TNF-α-dependant activation. 3D10 and PFAAP5 could be inhibiting NF-κB activation through one or more of the other stimuli.

We investigated the effect of 3D10 expression on cell viability because NF-κB has been linked to apoptosis as pro- and sometimes anti-apoptotic.[68-71] And since hOSCAR has been reported to enhance the survival of DCs,[74] we proposed an opposing function of 3D10. 3D10 and PFAAP5 did not have any effect on cell viability or TNF-α-dependant apoptosis. It would be interesting to investigate the effect of other apoptotic stimuli on 3D10 or PFAAP5 over-expressing cells.

A major finding should be addressed here. The cloned 3D10 in pcDNA3.1/His has been shown to be localized in the cytoplasm but at a later stage of 3D10 investigation it has been shown to be secreted. Sequence analysis of cloned 3D10 translated product (including the N-terminus tag) showed no signal peptide and possible membrane-bound product. Its cytoplasmic expression could be explained by the over-expression nature and/or the blockage of the N-terminus signal peptide by the His tag and Xpress epitope of the vector. This change of protein structure might have affected its folding, cleavage and secretion. Consequently, its function and behavior could have also been affected.

In conclusion, 3D10 and PFAAP5 inhibit NF-κB activity through TNF-α-independent pathway. Neither 3D10 nor PFAAP5 have any effect on cell viability or TNF-α-dependent apoptosis.

Figures

Figure 2.1. 3D10 inhibits NF-κB activity in a dose-response effect.

HEK 293T cells were plated in 12-well plate at a density of 7.5 x 10^4 and allowed to adhere for 24 h. The approximately 70-80% confluent cells were transiently transfected with 75 ng/ml 3X-κB-luc (Luc) with or without the following plasmids at the indicated concentration: 3D10 in pcDNA3.1/His, IκB-α super-repressor (negative control), or 75 ng/ml p65 (positive control). As control for transfection efficiency, β-Gal construct was used for all wells (75 ng/ml). Total DNA was maintained by adding the appropriate blank vector if needed. 48 h post-transfection, cell lysates were collected and processed for luciferase and β-Gal activities and read in a luminometer and plate reader respectively. The experiment was performed in triplicates. The averages were normalized and compared using Student's *t*-test. The luciferase activity of 3X-κB-luc-transfected cells was used as the reference and was arbitrarily set to 1.0. The experiment is a representative of three independent experiments carried out in triplicate. Bars represent standard deviations. * Statistically significant ($p < 0.05$).

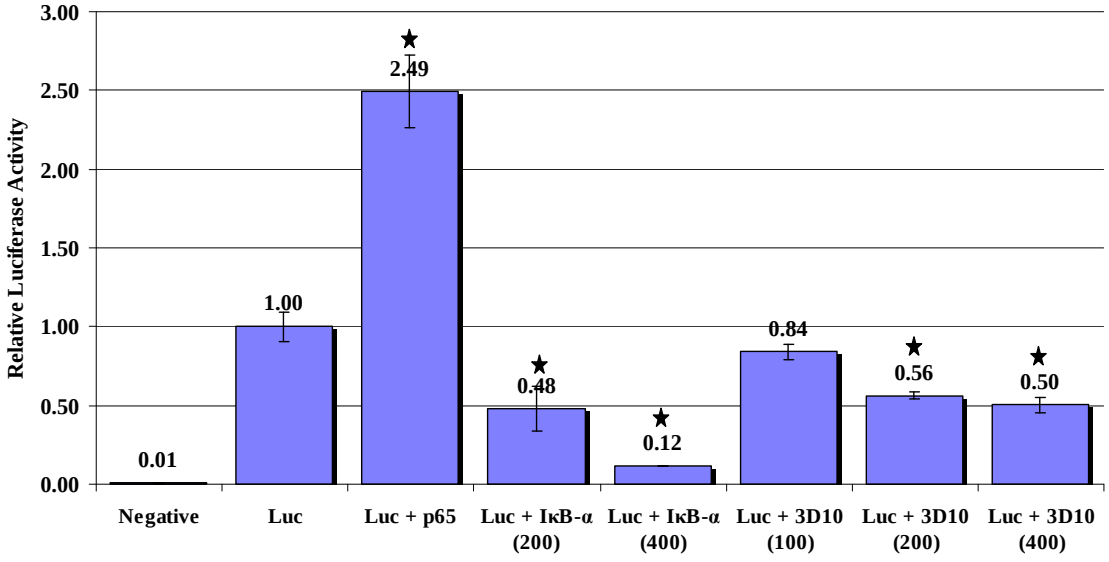

Figure 2.2. Both 3D10 and PFAAP5 inhibit NF-κB activity with the same efficiency. HEK 293T cells were plated in 12-well plate at a density of 7.5 x 10^4 and allowed to adhere for 24 h. The approximately 70-80% confluent cells were transiently transfected with 75 ng/ml 3X-κB-luc (kB-Luc) with or without the following plasmids at the indicated concentration: 3D10 in pcDNA3.1/His, p65 (positive control), IκB-α super-repressor (negative control), or PFAAP5 in pFLAG-CMV-4. As control for transfection efficiency, β-Gal construct was used for all wells (75 ng/ml). Total DNA was maintained by adding the appropriate blank vector if needed. 48 h post-transfection, cell lysates were collected and processed for luciferase and β-Gal activities and read in a luminometer and plate reader respectively. The experiment was performed in triplicates. The averages were normalized and compared to the luciferase activity of 3X-κB-luc-transfected cells which was used as the reference and was arbitrarily set to 1.0. The experiment is a representative of three independent experiments carried out in triplicate. Bars represent standard deviations.

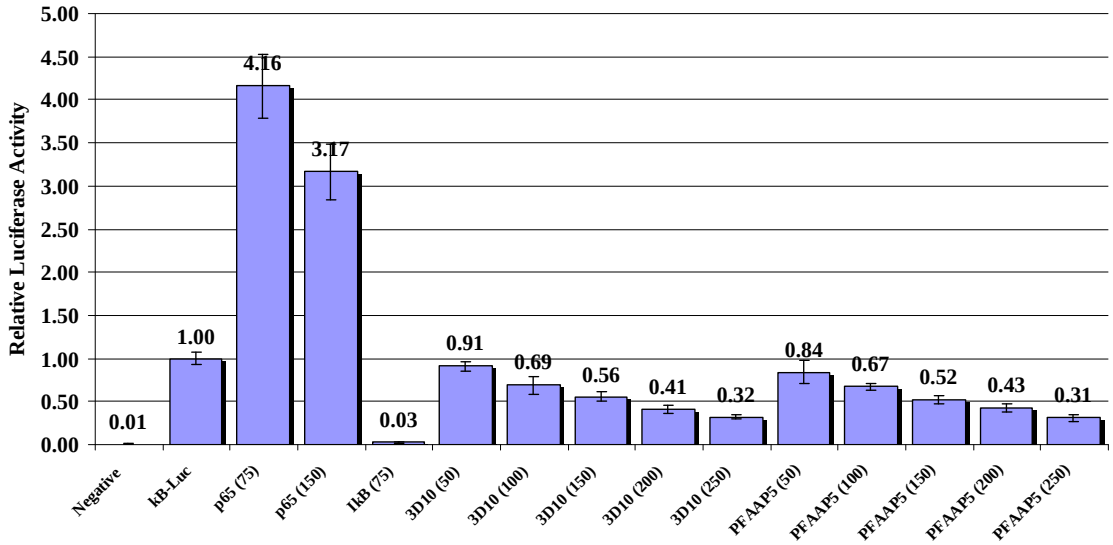

Figure 2.3. 3D10 is more efficient inhibitor to NF-κB activity than URP2.

HEK 293T cells were plated in 12-well plate at a density of 7.5 x 10^4 and allowed to adhere for 24 h. The approximately 70-80% confluent cells were transiently transfected with 75 ng/ml 3X-κB-luc (kB-Luc) with or without the following plasmids at the indicated concentration: 3D10 in pcDNA3.1/His, p65 (positive control), IκB-α super-repressor (negative control), or URP2 in pFLAG-CMV-4. As control for transfection efficiency, β-Gal construct was used for all wells (75 ng/ml). Total DNA was maintained by adding the appropriate blank vector if needed. 48 h post-transfection, cell lysates were collected and processed for luciferase and β-Gal activities and read in a luminometer and plate reader respectively. The experiment was performed in triplicates. The averages were normalized and compared to the luciferase activity of 3X-κB-luc-transfected cells which was used as the reference and was arbitrarily set to 1.0. The experiment is a representative of three independent experiments carried out in triplicate. Bars represent standard deviations.

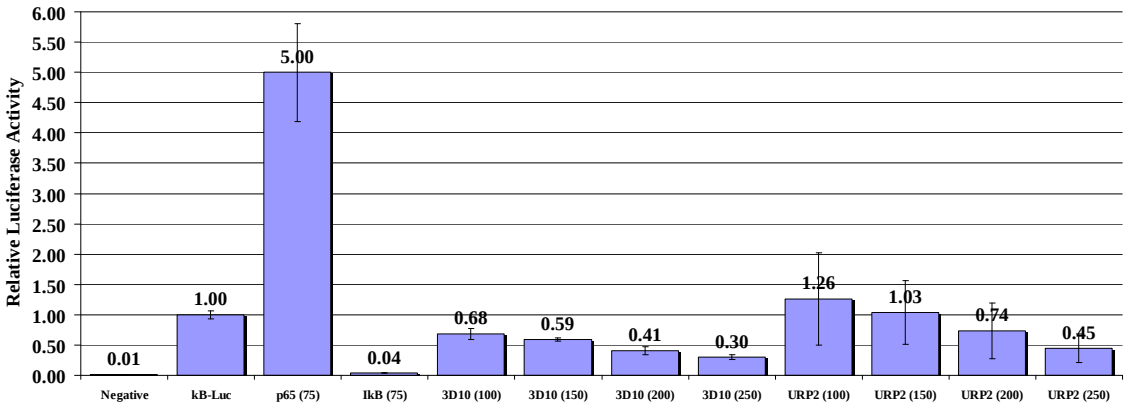

Figure 2.4. TNF failed to activate NF-κB but 3D10 showed significant inhibition. HEK 293T cells were plated in 12-well plate at a density of 7.5 x 10^4 and allowed to adhere for 24 h. The approximately 70-80% confluent cells were transiently transfected with 75 ng/ml 3X-κB-luc and 100 ng/ml of either 3D10 in pcDNA3.1/His or the empty vector. As control for transfection efficiency, β-Gal construct was used for all wells (75 ng/ml). 24 h post transfection, cells were either stimulated or not stimulated with human recombinant TNF-α (10 ng/ml) for 30 min. Cell lysates were collected and processed for luciferase and β-Gal activities and read in a luminometer and plate reader respectively. The experiment was performed in duplicates. The averages were normalized and compared to the luciferase activity of empty vector-transfected cells which was used as the reference and was arbitrarily set to 1.0. The experiment is a representative of three independent experiments carried out in duplicates. Bars represent standard deviations.

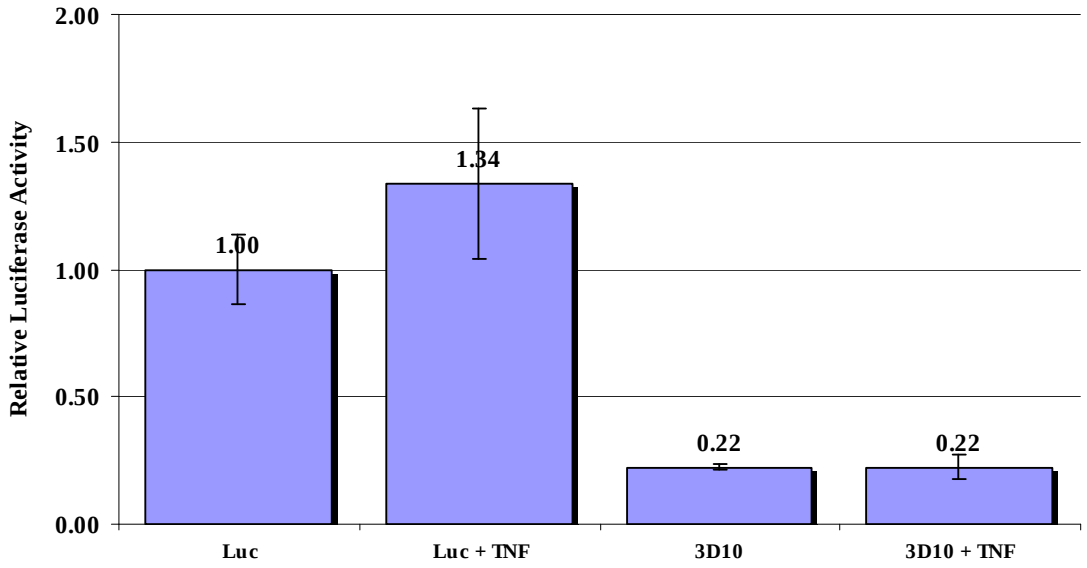

Figure 2.5. 3D10 failed to inhibit TNF-dependent NF-κB activation.

HEK 293T cells were plated in 12-well plate at a density of 7 x 10^4 and allowed to adhere for 24 h. The approximately 70% confluent cells were transiently transfected with 100 ng/ml 3X-κB-luc and 100 ng/ml of either 3D10 in pcDNA3.1/His or the empty vector. As control for transfection efficiency, β-Gal construct was used for all wells (100 ng/ml). 5 h post-transfection, culture media was exchanged with fresh media. 24 h post transfection, cells were either stimulated or not stimulated with human recombinant TNF-α (10 ng/ml) for 12 h. Cell lysates were collected and processed for luciferase and β-Gal activities and read in a luminometer and plate reader respectively. The experiment was performed in duplicates. The averages were normalized and compared to the luciferase activity of empty vector-transfected cells which was used as the reference and was arbitrarily set to 1.0. The experiment is a representative of three independent experiments carried out in duplicates. Bars represent standard deviations.

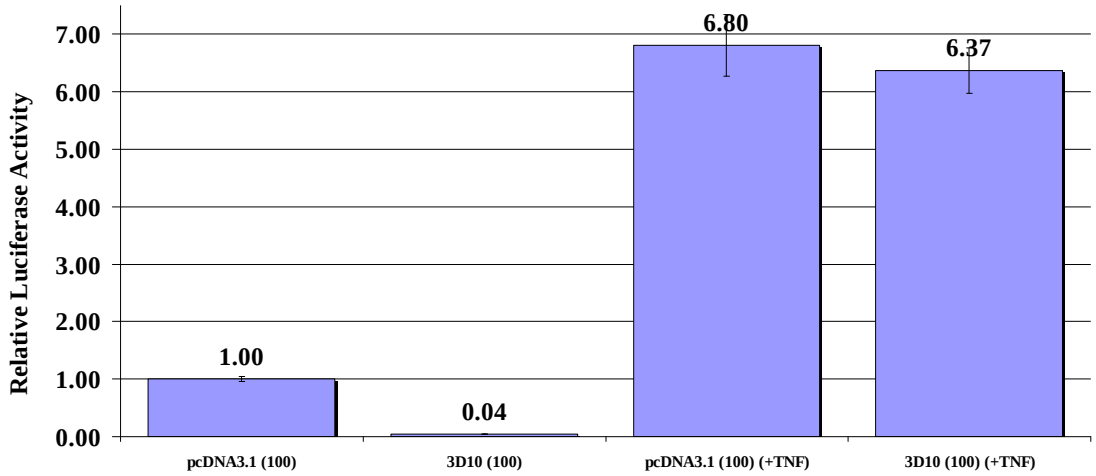

Figure 2.6. 3D10 and PFAAP5 show and additive effect in NF-κB inhibition.

HEK 293T cells were plated in 12-well plate at a density of 7.5 x 10^4 and allowed to adhere for 24 h. The approximately 70-80% confluent cells were transiently transfected with 75 ng/ml 3X-κB-luc with or without the following plasmids: IκB-α super-repressor (75 ng/ml), 3D10 in pcDNA3.1/His (100 ng/ml), PFAAP5 in pFLAG-CMV-4 (100 ng/ml), or both 3D10 and PFAAP5 (100 ng/ml each). As control for transfection efficiency, β-Gal construct was used for all wells (75 ng/ml). Total DNA was maintained by adding the appropriate blank vector. 48 h post-transfection, cell lysates were collected and processed for luciferase and β-Gal activities and read in a luminometer and plate reader respectively. The experiment was performed in triplicates. The averages were normalized and compared to the luciferase activity of 3X-κB-luc-transfected cells which was used as the reference and was arbitrarily set to 1.0. The experiment is a representative of three independent experiments carried out in triplicate. Bars represent standard deviations.

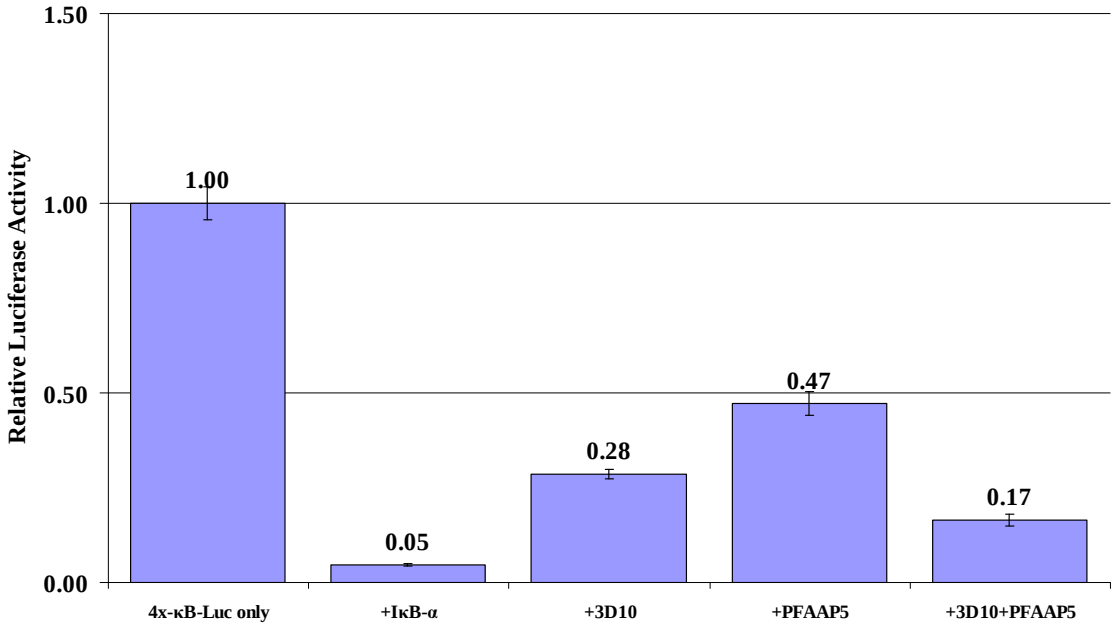

Figure 2.7. 3D10 and PFAAP5 showed no effect on cell viability.

HEK 293T cells were seeded in 96-well plates at 3 x 10^4 cells/well in 100 µl culture media. Cells were transfected with different plasmids at different concentrations as indicated. 24 h post-transfection, cells in one plate were processed for baseline reading and cells in another plate were stimulated with 30 ng/ml TNF-α in fresh media for 24 h to induce apoptosis and then processed as follows: 20 µl of CellTiter reagent was added to each well and the plate was incubated at 37°C and 5% CO_2 for 1 h. Soluble formazan produced by viable cellular reduction was measured by recording the absorbance at 490 nm using a 96-well plate reader. All wells were in triplicates and averages were compared.

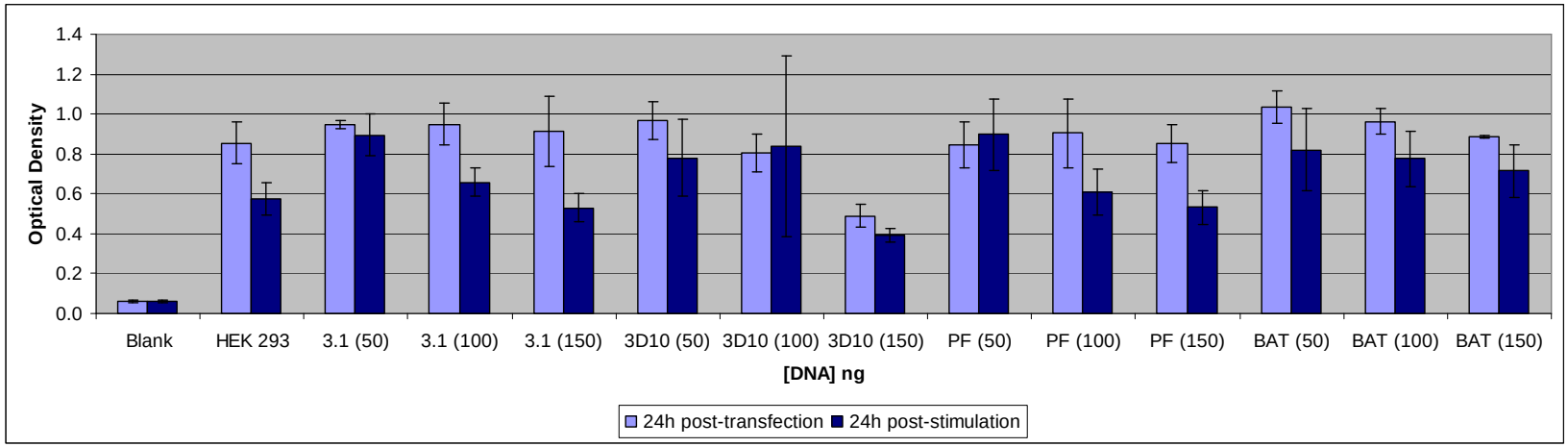
Optical Density
1.4
1.2
1.0
0.8
0.6
0.4
0.2
0.0
Blank
HEK 293
3.1 (50)
3.1 (100)
3.1 (150)
3D10 (50)
3D10 (100)
3D10 (150)
PF (50)
PF (100)
PF (150)
BAT (50)
BAT (100)
BAT (150)
[DNA] ng
24h post-transfection
24h post-stimulation

Chapter 3. Searching For 3D10-Binding Partners Using the Yeast Two Hybrid Screening

Background

3D10 appears to be a soluble protein. It appears also to be secreted which suggests a decoy receptor role. Identifying 3D10 binding partner(s) is very important. Due to the difficulty of testing all potential partners individually, it has been a common research method to use the yeast-two hybrid screening. It is a well-established and reliable method if used and interpreted properly. Identified binding partners to 3D10 could be different ligands or intra-cellular signaling molecules and trafficking regulators. Here we performed two rounds of the yeast-two-hybrid screening of mouse calvaria and human macrophage cDNA libraries each one separately, and identified several potential binding partners to 3D10. This list of proteins has the potential to open many venues in the future to further study OSCAR.

Materials and Methods

Library and Prey Construction – A macrophage cDNA library (Clontech) was used to construct the yeast library (prey) using MATCHMAKER Library Construction & Screening Kit (Clontech) which will be described briefly here. 20 µl cDNA and 5-6 µl vector pGADT7-Rec (yeast Gal4 activation domain (AD) vector) (Clontech) were co-transformed into AH109 *Saccharomyces cerevisiae* yeast strain using lithium acetate (LiAc)-mediated protocol. 150 µl of 1:1000 dilution of the co-transformation mixture was spread on a

Synthetic Defined media (SD)/-Leu plate to check the transformation efficiency. The remaining 15 ml transformants was spread on 100 SD/-Leu plates. After incubation at 30ºC for 3-6 days until colonies appeared, the transformants were harvested with freezing medium and the concentration was adjusted to 6 x 10^6 cells/ml. Aliquots of 1 ml were made and tubes stored at -80ºC.

The mouse calvaria library was constructed using the MATCHMAKER library construction & screening kit (Clontech) following the manufacturer's instructions and is descried briefly here. The calvaria of 7-day old mouse pups was dissected and placed in DEPC-treated ice-cold PBS. All adherent soft tissues were carefully removed before placing the tissues in Guanidine-HCl buffer. Total RNA was isolated using the cesium chloride gradient centrifugation method.[47] The RNA pellet was washed thoroughly before re-suspension. 100 µg of total RNA was used to isolate the mRNA using Straight A's mRNA isolation system (Novagen). One mg of mRNA was reverse transcribed with MMLV reverse transcriptase and primed with oligo d(T) primer and SMART III oligonucleotide. After first-strand cDNA was synthesized, long distance-PCR was used to amplify the double strand cDNA. The double strand PCR product was then loaded on 1% agarose gel. Only cDNA larger than 800 bp in size was cut out and purified using QIAEX II gel extraction kit (Qiagen). Then 20 µl dscDNA and 6 µl vector pGADT7-Rec were co-transformed into yeast AH109 using LiAc-mediated protocol. 150 µl of the 1:1000 dilution of the co-transformation mixture was spread on a 150-mm SD/-Leu to check the transformation efficiency. The remaining 15 ml transformants were spread on 100 150-mm SD/-Leu plates. After incubation at 30ºC for 3-6 days until colonies appear, the transformants were harvested with freezing medium and the concentration was 6 X 10^7 cells/ml. The transformation efficiency was > 1.5

X 10^6 transformants / 3 µg pGADT7-Rec. Aliquots of 1 ml were made and tubes stored in -80ºC freezer.

Bait Construction – 3D10 full coding cDNA was cloned into the bait vector pGBKT7 (yeast Gal4 DNA-binding domain (DNA-BD) fusion protein vector) and used to transform the *Saccharomyces cerevisiae* yeast strain Y187. The bait plasmid was first tested for activity and/or toxicity. The plating was repeated as it was done for the library but using SD/-Trp and no harvesting was needed.

Yeast mating – SD agar plates were prepared: four 100-mm plates for each SD/–Leu, SD/–Trp, and SD/–Leu/–Trp; and fifty 150-mm plates SD/–Ade/–His/–Leu/–Trp. A concentrated overnight culture of Y187 bait colony was combined with 1 ml aliquot of AH109 library for mating. The mating culture was incubated at 30°C for 24 h. Zygotes presence was checked just before the end. The mating mixture was collected carefully and centrifuged. The cell pellet was re-suspended and plated. To determine the mating efficiency, 100 µl of a 1:10,000, 1:1,000, 1:100, and 1:10 dilution of the mating mixture was spread on three media (100-mm plates): SD/–Leu, SD/–Trp and SD/–Leu/–Trp. The remaining mating mixture was spread on SD/–Ade/–His/–Leu/–Trp plates (200 µl cells/150-mm plate). The plates were incubated at 30°C for 10-15 days. Positive colonies (>100) were harvested for plasmid DNA extraction.

Electrocompetent E. coli Preparation – LB media with low salt concentration was prepared in large quantity and stored at room temperature. 100 ml ice cold 10% glycerol was filter

sterilized. *E. coli* DH5α cells (Invitrogen) were inoculated in 3 ml of media and grown at 37°C for 12-16 h at 250 rpm shaking. Four 500 ml of LB in flasks were inoculated with 500 µl of overnight culture and incubated at 37°C while shaking vigorously at 250-300 rpm to an OD600 of 0.6-0.8. Flasks were transferred to ice when the cells reached the correct optical density and held for 15 min. 330 ml of the cells was transferred to 6 ice-cold sterile 500 ml centrifuge bottles and centrifuged at 4000 x *g* for 15 min. Media was discarded and cells were kept on ice at all times. Cells were gently suspended in one-volume sterile ice-cold distilled water (dH_2O) and centrifuged at 4000 x *g* at 4°C for 15 minutes. The second and third washes were done in 0.5 volumes of sterilized ice-cold H_2O. The 4th and 5th (final) washes were done in 0.02 volumes of sterilized ice-cold H_2O and filter-sterilized ice-cold 10% glycerol respectively. Transformation efficiency was tested and aliquots of 250 µl were quickly frozen in a dry ice/ethanol bath in microfuge tubes and stored at -80°C until required.

Plasmid DNA Isolation and Sequencing – yeast plasmids were isolated using the yeast plasmid protocol. Briefly, colonies were cultured in liquid medium overnight. Cell pellets were processed and lysed. Different reagents were used with freezing and finally plasmid pellets were suspended in dH_2O. Electrocompetent *E. coli* KC8 (Clontech) or DH5α (prepared locally) were transformed with 30 yeast plasmids from the first round and 50 from the second using cuvettes and Electroporation device and method. Cells were plated on LB/amp agar medium and incubated at 37°C for 24 h. One colony from each plate was cultured and its respective plasmid DNA was isolated using QIAprep miniprep kit (Qiagen). Isolated plasmid DNAs were sent for sequencing at UNC genome analysis facility. Sequences were analyzed with BLAST program (NCBI).

Co-transformation – The first step of binding confirmation was performed by yeast co-transformation. Selective plasmids were tested for binding with 3D10 by co-transformation with pGBKT7-3D10 plasmid into AH109 yeast and were plated on a selection medium (SD/–Ade/–His/–Leu/–Trp/X-Gal). Selection media plates were plated with 3D10 only, plasmid of interest only and both together. Positive growth of the co-transformed yeasts only indicates true binding.

Confocal Laser Microscopy Co-localization – Rat bone marrow cells were isolated. Femora and tibiae were aseptically removed and dissected free of adherent soft tissues. The bone ends were cut, and the marrow cavity was flushed out with α-MEM medium (Sigma-Aldrich) from one end of the bone using a sterile 21-gauge needle. The bone marrow suspension was carefully dispersed to obtain a single-cell suspension. The cells were washed twice and re-suspended (10^6 cells/ml) in α-MEM containing 10% FBS, and added to 12-well plates containing glass coverslips. M-CSF (30 ng/ml) and RANKL (30 ng/ml) were added to induce OC formation. Cultures were fed on day 3 by fresh medium and reagents. After incubation for 5 days, coverslips were washed twice with PBS, fixed with 3.7% formalin in PBS for 10 min, washed twice in TBS and permeabalized in 0.5% Triton X for 10 min and then washed in TBS-Tween 20. They were then blocked with 1% BSA in PBS for 20 min (all steps were performed at 4°C). Cells were treated with primary Ab (rabbit Anti-3D10 anti-sera and chicken anti-actin Ab) for 60 min at 37°C, washed, and treated with secondary FITC- or Texas Red-labeled Abs (Jackson ImmunoResearch Laboratories) for 60 min. Cells were

washed twice with PBS-Tween 20 and viewed with Zeizz LSM5 Pascal Confocal Laser Scanning Microscope (Zeiss, Germany).

HEK 293T or RAW 264.7 cells were plated on glass coverslips in 12-well plates and allowed to adhere for 24 h. Using the Effectene transfecting kit (Qiagen), cells were co-transfected with 3D10 plasmid (pcDNA3.1/His) and either PFAAP5 or BAT3 plasmid (pFLAG-CMV-4). 24 h post-transfection, cells were fixed and stained as previously described using mouse Anti-Xpress Ab (Invitrogen) for 3D10 and rabbit Anti-FLAG Ab (Sigma) for either PFAAP5 or BAT3.

Actin Binding Assay – To confirm actin binding without IP, an actin binding spin-down assay kit (Cytoskeleton, Inc.) was used. This assay depends on co-sedimentation of actin and the binding partner (3D10) in the pellet compared to the supernatant. The positive control is α-Actinin and the negative control is BSA. The assay was performed according to the manufacturer's instructions. Briefly, 3D10 and the control proteins were incubated with 40 µg of freshly polymerized actin (F-actin) for 1 h at room temperature. After incubation, each protein plus F-actin solution was subject to high-speed centrifugation (160,000 x *g*) to pellet F-actin and protein bound to it. The pellet fraction was dissolved in SDS-sample buffer, the volume being equal to the initial incubation volume. Equivalent volumes of pellet and supernatant fractions were analyzed by SDS-PAGE followed by Coomassie blue staining.

Results

Over 200 yeast colonies positively grew in the highest stringency setting in each round of the screening. Out of these, we sequenced over 80 plasmids; approximately 30 from 1st round

and 50 from 2nd round (Table 3.1). The results from the first round were over 70% actin. From the 2nd round, we observed only 7 that have multiple (2-4) hits and two from the same family (Table 3.2). Actin and two other genes were investigated further according to their relevance to 3D10 characterization. Target genes were genes with multiple hits especially cytoplasmic proteins-encoding genes, and receptors that may signal through 3D10 binding.

Actin from the 1st round and 12 plasmids from the second were tested. Actin and 7 plasmids were confirmed (Figure 3.1). Actin, PFAAP5 and BAT3 were screened for co-localization with 3D10. PFAAP5 and BAT3 are nuclear proteins. While PFAAP5 is of unknown function, BAT3 is known to be an apoptosis regulator.[67] Since OSCAR has been reported to be anti-apoptotic in DCs,[74] we hypothesized that 3D10 may play an opposite role by binding to nuclear proteins and apoptotic regulators. 3D10 detection was done with either anti-Xpress mAb or anti-3D10 polyclonal Ab that show almost identical images (Figure 3.2). PFAAP5 and BAT3 clones were purchased from OriGene and cloned into pFLAG-CMV-4 expression vector (Sigma) with an N-terminus FLAG epitope.

Actin showed a typical cytoskeleton distribution while 3D10 showed the main distribution perinuclear and at the plasma membrane. The co-localization was minimal and mainly at the plasma membrane region (Figure 3.3). PFAAP5 and BAT3 were nuclear and co-localization was not conclusive from these slides (Figure 3.4).

Actin binding assay showed that 3D10 precipitated with actin suggesting positive binding. Suspended 3D10 with no actin showed some precipitation as well (Figure 3.5).

Discussion

Yeast-two-hybrid system can result in a wide range of interactions; few vs. too many, weak vs. strong, and true vs. false interactions. Few, strong and true interactions are of our interest. To minimize the number of colonies to exclude weak and false interactions, we used a high stringent selection medium.

At the time the yeast-two hybrid screening was performed, 3D10 was considered a cytoplasmic protein. The 1st round was designed to pick cytoplasmic binding partners from mouse bone tissues. The results showed actin as the majority hits which indicated a true interaction at least at the *in vitro* level. Actin seemed to be of interest because of this number of hits and because of its relevance to actin ring formation of activated OCs.[75] The complete investigation of actin binding was faced by many pitfalls. Co-immuno-precipitation was difficult to be resolved due to actin size (approximately 45 kDa) which overlaps the heavy chain of IgG in western blot. Confocal microscopy showed some co-localization at the plasma membrane. Actin binding assay was not conclusive because 3D10 could not be purified in sufficient amount to perform this assay with good control. At this stage we moved to the second round looking for human binding partners to the full 3D10 molecule. We used MΦ cDNA library because of 3D10 expression in these cells and to limit the search in a smaller field of tissues.

Nuclear proteins binding could not be co-localized with 3D10 in immuno-fluorescence studies. Their binding could be confirmed by Co-IP and fractionation of cell lysates into nuclear and cytoplasmic extracts looking for any change in protein localization with double transfection.

Target proteins have been changed after 3D10 was found to be secreted. Candidate proteins now could be ligands, trafficking modulators, or transcription factors. Among the interesting results we found are Major histocompatibility complex, class I (MHC I), C (HLA-C), one membrane-bound ligand (Lymphotoxin beta (LTB), also known as TNF superfamily, member 3), and some nuclear proteins (Phosphonoformate immuno-associated protein 5 (PFAAP5), Human Leukocyte Antigens-B (HLA-B)-associated transcript 3 (BAT3) and some transcription factors). It is known for members of LRC to bind to MHC I as ligands.[30,33] MHC I molecules could be ligands for OSCAR. Other possibilities are LTB and membrane-bound proteins. mOSCAR ligand has been proposed to be expressed on osteoblast surface like RANKL.[43] Nuclear proteins are interesting because of the potential role in regulating cell differentiation, survival and activation of immune response.

Although 3D10 has the potential to polymerize, we did not find any supporting evidence among the 50 plasmids that we sequenced.

These results will be analyzed in the future 3D10 research by functional analysis and comparing *in vivo* binding to different OSCAR isoforms. Functional analyses include Co-IP, co-localization and modulation of known OSCAR function.

Other alternatives to the yeast-two-hybrid screening are the Tandem Affinity Purification, Phage Display and Protein Chips (or Protein Micro-Array). These methods require pure protein (3D10) which was not available at the time of the present study. And the first method requires also protein engineering before its expression and purification.

In conclusion, none of the selected candidates was completely confirmed to bind to 3D10. Several strong candidates have been identified some of which are under investigation. The future of 3D10 and hOSCAR study is dependent on the identification of its ligand(s) and

modulator(s).

Tables

Table 3.1. Sequencing results of the yeast-two-hybrid screening of the macrophage cDNA library.

No.	Y2H ID	Name	Nucleotide ID	Protein ID	Tested	Confirmed
1	1	Ubiquitously-expressed transcript (UXT), transcript variant 1/2	NM_153477 NM_004182	NP_705582 NP_004173	Yes	No
2	2	Ficolin (collagen/fibrinogen domain containing) 1 (FCN1)	NM_002003	NP_001994	No	No
3	3	Clone	AY358502	AAQ88866	No	No
4	4	Flotillin 2 (FLOT2)	NM_004475	NP_004466.1	No	No
5	5	Heterogeneous nuclear ribonucleoprotein F (HNRPF)	NM_004966	NP_004957.1	Yes	Yes
6	6	Chitinase 1 (chitotriosidase) (CHIT1)	NM_003465	NP_003456.1	Yes	Yes
7	7	UNC-112 related protein 2 (URP2)	NM_178443 NM_031471	NP_848537 NP_113659	Yes	Yes
8	8	Phosphonoformate immuno-associated protein 5 (PFAAP5)	NM_014887	NP_055702	Yes	Yes
9	9	Hypothetical protein LOC91289	NM_033200	NP_149977.1	Yes	Yes
10	10	Same as #7	NM_178443		Yes	Yes
11	11	Same as #8	NM_014887		Yes	Yes
12	12	Histidine triad nucleotide binding protein 1 (HINT1)	NM_005340	NP_005331	Yes	Yes
13	13	Calcium channel, voltage-dependent, beta 1 subunit, transcript variant 1	BC037311	AAH37311	Yes	No
14	14	S100 calcium binding protein A9 (calgranulin B)	BC047681 NM_002965	AAH47681 NP_002956	Yes	No
15	15	Human Leukocyte Antigens-B (HLA-B) associated transcript 3 (BAT3), transcript variant 1	NM_004639	NP_004630	Yes	Yes
16	16	Similar to Actin	AK125561		No	No

17	17	Same as #8	NM_014887		Yes	Yes
18	18	XXX	AC004264		No	No
19	19	XXX	AL807752		No	No
20	20	Hermansky-Pudlak syndrome protein (HPS)	U65676	AAB17869	Yes	No
21	23	BTG family, member 2 (BTG2)	NM_006763	NP_006754	No	No
22	24	RAB43, member RAS oncogene family (RAB43)	NM_198490	NP_940892 (RAB41)	No	No
23	26	Lymphotoxin beta (TNF superfamily, member 3) (LTB), transcript variant 2	NM_009588	NP_033666	No	No
24	28	Chitobiase, di-N-acetyl- (CTBS)	NM_004388	NP_004379	No	No
25	29	Pellino homolog 1 (Drosophila) (PELI1)	NM_020651	NP_065702	No	No
26	32	PAC clone RP1-102K2 from 22q12.1-qter	AC004264		No	No
27	34	DnaJ (Hsp40) homolog, subfamily A, member 3 (DNAJA3)	NM_005147	NP_005138	No	No
28	51	Benzodiazapine receptor (peripheral) (BZRP), transcript variant PBR OR PBR-S	NM_000714 NM_007311	NP_000705 NP_009295	No	No
29	52	Glutamate-ammonia ligase (glutamine synthase) (GLUL)	NM_002065	NP_002056	No	No
30	53	Human DNA sequence from clone RP11-440G5 on chromosome 9 Contains the NFIL3 gene for interleukin 3 regulated nuclear factor, a novel gene and two CpG islands	AL353764	CAH73854	No	No
31	54	Heterogeneous nuclear ribonucleoprotein H1 (H) (HNRPH1) See #5	NM_005520	NP_005511	No	No
32	55	Same as #8			Yes	Yes
33	56	Same as #14			Yes	No
34	57	BAC clone RP11-383I5 from 2	AC019201	AAY14898	No	No
35	58	Same as #7			Yes	No
36	59	Hypothetical protein	NM_017730	NP_060200	No	No

		LOC54870				
37	60	Myosin, heavy polypeptide 9, non-muscle (MYH9)	NM_002473	NP_002464	No	No
38	61	Maltase-glucoamylase (alpha-glucosidase) (MGAM)	NM_004668	NP_004659	No	No
39	62	Family with sequence similarity 48, member A (FAM48A), transcript variant 2	NM_017569	NP_060039	No	No
40	63	CD27-binding (Siva) protein (SIVA), transcript variant 1	NM_006427	NP_006418	No	No
41	64	Major histocompatibility complex, class I, C (HLA-C)	NM_002117	NP_002108	No	No
42	65	Nuclear factor (erythroid-derived 2)-like 2 (NFE2L2)	NM_006164	NP_006155.2	No	No
43	66	Same as #7			No	No
44	67	Pyruvate kinase, muscle (PKM2), transcript variant 1, 2 & 3	NM_002654 NM_182470 NM_182471		No	No
45	69	Interleukin 2 receptor, beta (IL2RB)	NM_000878	NP_000869.1	No	No
46	70	Same as #26	NM_009588		No	No
47	71	Same as #29	NM_020651		No	No
48	72	Cytochrome P450, family 2, subfamily S, polypeptide 1 (CYP2S1)	NM_030622	NP_085125.1	No	No
49	74	Same as #15	NM_004639		No	No
50	75	Same as #51	NM_000714 NM_007311		No	No

Table 3.2. Summary of the multiple hits from table 3.1.

Protein	Y2H ID
Heterogeneous nuclear ribonucleoprotein F (HNRPF) Heterogeneous nuclear ribonucleoprotein H1 (H) (HNRPH1)	5, 54
UNC-112 related protein 2 (URP2)	7, 10, 58, 66
Phosphonoformate immuno-associated protein 5 (PFAAP5)	8, 11, 17, 55
S100 calcium binding protein A9 (calgranulin B)	14, 56

HLA-B associated transcript 3 (BAT3), transcript variant 1	15, 74
Lymphotoxin beta (TNF superfamily, member 3) (LTB), transcript variant 2	26, 70
Pellino homolog 1 (Drosophila) (PELI1)	29, 71
Benzodiazapine receptor (peripheral) (BZRP), transcript variant PBR OR PBR-S	51, 75

Figures

Figure 3.1. Co-transformation of actin with 3D10 bait vector.

Isolated plasmids from the binding partners were co-transformed with pGBKT7-3D10 plasmid into AH109 yeast and were plated on a selection medium (SD/–Ade/–His/–Leu/–Trp/X-Gal). Each plate was plated with 3D10 only, plasmid of interest only and both together. Neither 3D10 (1) nor the binding partner (actin) (2) grows. Positive growth of the two plasmids co-transformation indicates positive protein-protein interaction (3).

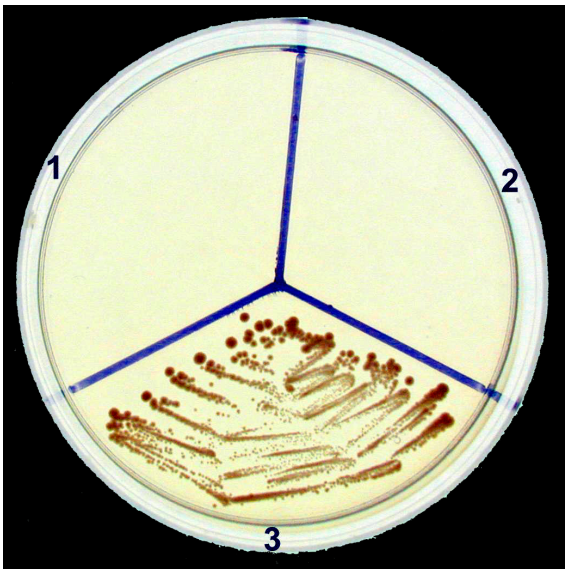

Figure 3.2. Immuno-fluorescence of transiently transfected cells shows that 3D10 localizes in the cytoplasm.

HEK 293T (top) or RAW 264.7 (bottom) cells were plated in low density on glass coverslips. Cells were transiently transfected with 3D10 plasmid (pcDNA3.1/His). Transfected cells were fixed and stained as described using anti-Xpress Ab and Texas Red-labeled secondary

Ab (left), or anti-3D10 Ab and FITC-labeled secondary Ab (middle). 3D10 was localized in the cytoplasm by both antibodies. Merged images (right) show almost identical localization.

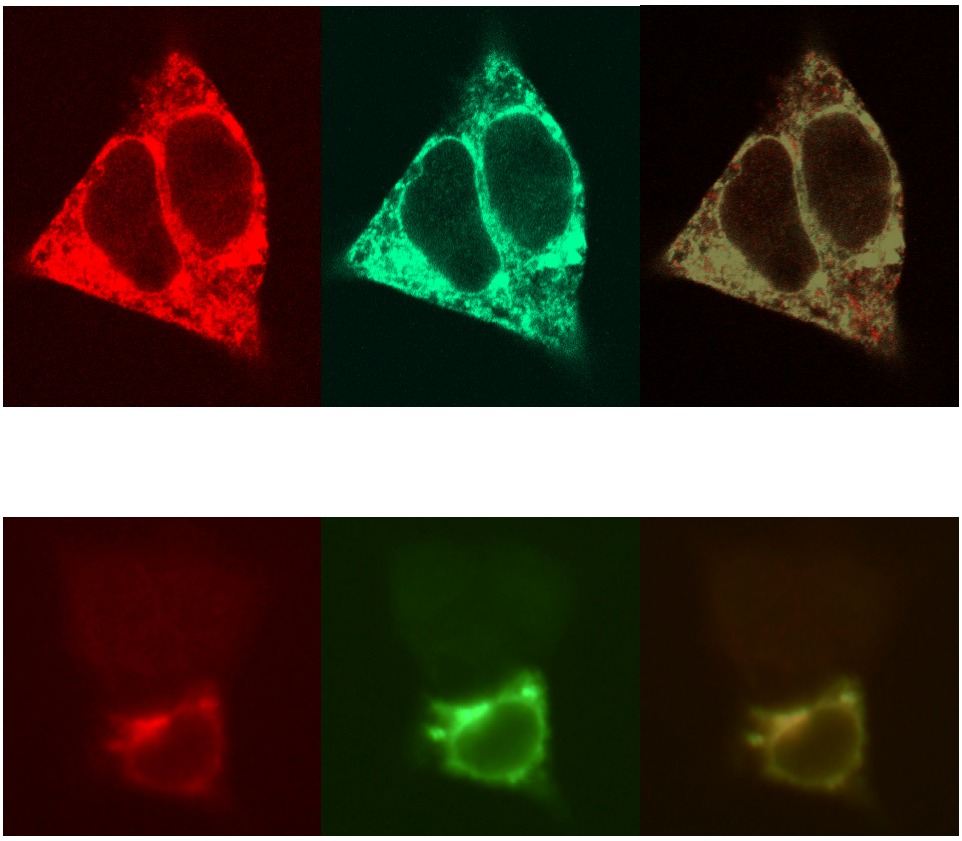

Figure 3.3. 3D10-Actin co-localization is minimal and mainly at plasma membrane. RBM cells were isolated and induced to differentiate into OC as described. Cells grown on coverslips were fixed and stained with anti-3D10 anti-sera and FITC-labeled secondary Ab, and anti-actin Ab and Texas Red-labeled secondary Ab. 3D10 (left), actin (middle) and merged images (right) show minimal co-localization mainly at the plasma membrane.

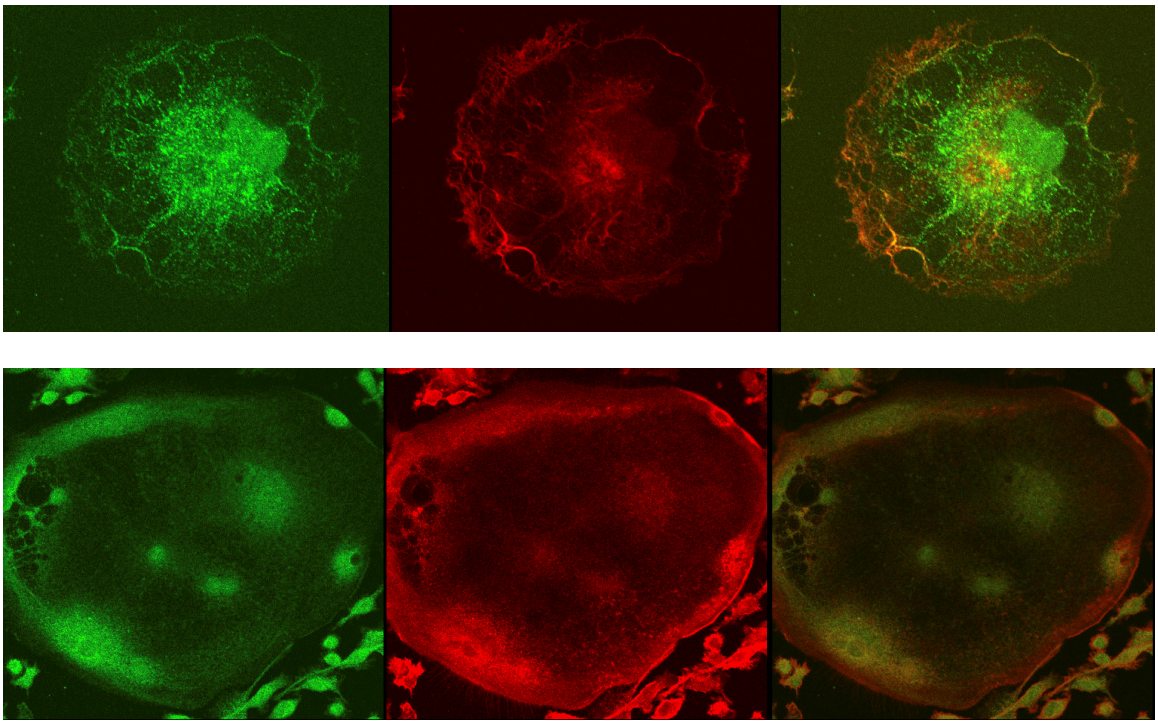

Figure 3.4. 3D10-Nuclear proteins co-localization.

HEK 293T or RAW 264.7 cells were plated on glass coverslips and allowed to adhere for 24 h. Cells were co-transfected with 3D10 plasmid (pcDNA3.1/His) and either PFAAP5 or BAT3 plasmid (pFLAG-CMV-4). 24 h post-transfection, cells were fixed and stained as previously described using mouse Anti-Xpress Ab and Texas Red-labeled secondary Ab for 3D10, and rabbit Anti-FLAG Ab and FITC-labeled secondary Ab for either PFAAP5 or BAT3. 3D10 (left) is cytoplasmic and PFAAP5 (middle top) and BAT3 (middle bottom) are nuclear. Merged images (right) show no co-localization.

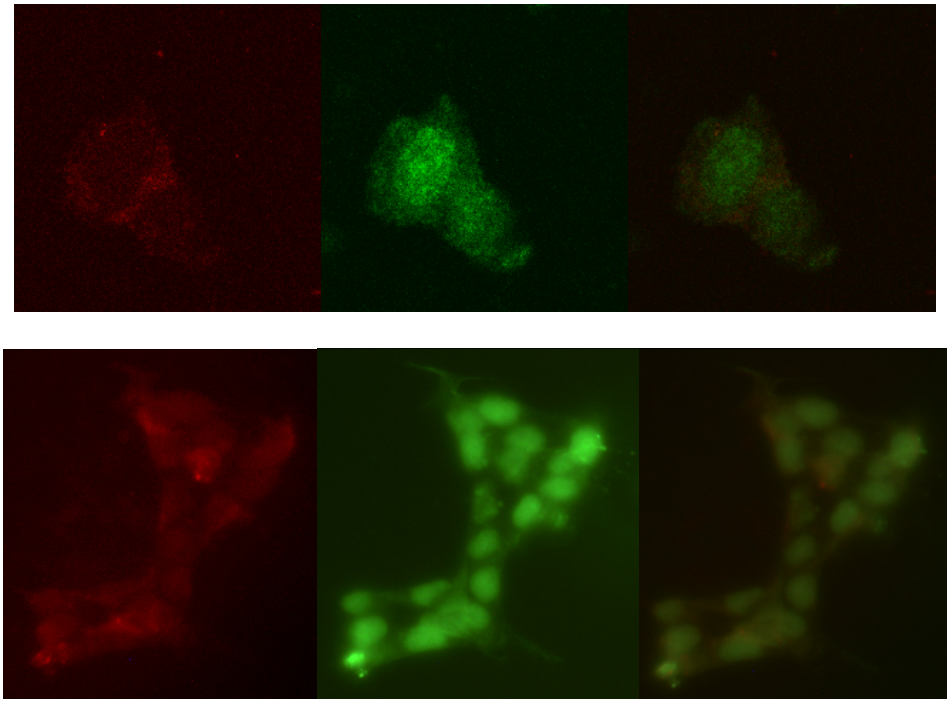

Figure 3.5. 3D10-Actin co-sedimentation assay.

Purified 3D10 or the control protein (positive control α-Actinin and the negative control BSA) was incubated with 40 µg of freshly polymerized actin (F-actin) for 1 h at room temperature. Each protein plus F-actin solution was subject to high-speed centrifugation (160,000 x *g*). The pellet fraction was dissolved in SDS-sample buffer. Equivalent volumes of pellet and supernatant fractions were analyzed by SDS-PAGE followed by Coomassie blue staining. Coomassie blue stained gel of the assay shows that 3D10 completely co-precipitated with actin but it also showed some precipitation without actin. The positive control α-Actinin co-precipitated with actin in the pellet (P) and the negative control BSA remained in the supernatant (SN).

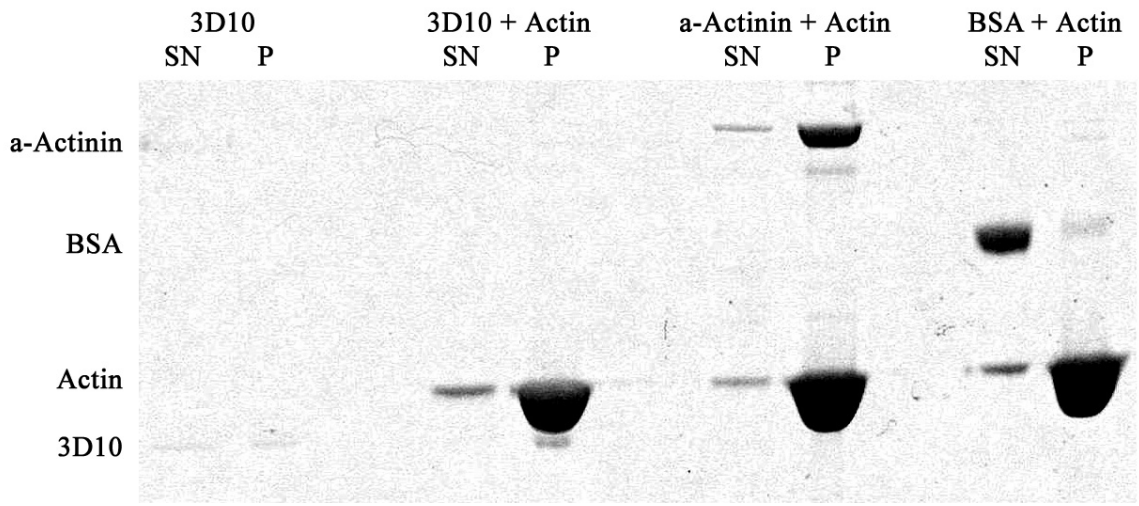
3D10
SN
P
3D10 + Actin
SN
P
a-Actinin + Actin
SN
P
BSA + Actin
SN
P
a-Actinin
BSA
Actin
3D10

Chapter 4. Identification of a Secreted Form of the Human Osteoclast-Associated Receptor (hOSCAR)

Abstract

Human osteoclast-associated receptor (hOSCAR) is a member of the leukocyte receptor cluster (LRC) for an unknown ligand. hOSCAR has been reported to be expressed in several mononuclear cells (MNC) of myeloid origin and plays a role in modulating innate and adaptive immune response. We identified an alternative spliced isoform of hOSCAR that we had originally named 3D10. Sequence analysis showed that hOSCAR is expressed as membrane-bound (hOSCARm) and soluble (hOSCARs) isoforms with a non-spliced intron resulting in larger transcripts and soluble proteins lacking the trans-membrane domain. The expression profiles and tissue distribution of hOSCARm and hOSCARs were compared using specific PCR primers and new antibodies made in rabbits against either all or hOSCARs isoforms. Both isoforms were found to be differentially expressed in a wide variety of tissues. They were also found to be expressed in all MNC and neutrophils. hOSCARm isoforms appeared to be down-regulated more than the hOSCARs isoforms following stimulation of MNC with the mitogens PWM, Con A and PHA. Studies using THP-1 cells showed that the soluble isoforms are secreted and are up-regulated by both PMA and LPS. In conclusion, hOSCARs isoforms represent novel secretory isoforms of hOSCAR that may be functioning as decoy receptors.

Introduction

Leukocyte function and differentiation are regulated by cell surface receptors. A group of gene families of these receptors are mapped on chromosome 19q13.42, forming the Leukocyte Receptor Cluster (LRC) [30] which is part of the Immunoglobulin Super-family (Ig-SF). These genes and gene families within this cluster include killer cell inhibitory receptors (KIR),[31] killer cell activatory receptors (KAR),[32] leukocyte Ig-like receptors (LIR) [33,34] also known as Ig-like transcripts (ILT),[35,36] monocyte/macrophage (myeloid) inhibitory receptors (MIR),[37] HM and HL clones,[38] CD85 [39] or Leukocyte Ig-like receptors (activating LILRA or inhibiting LILRB) according to the Human Genome Organization (HUGO) Gene Nomenclature Committee HGNC (http://www.gene.ucl.ac.uk/nomenclature/genefamily/lilr.php); human hematopoietic Fc receptor for IgA (FcαR),[40] and leukocyte-associated Ig-like receptors (LAIR).[41] The two largest families are the KIRs/KARs and the LILRs. They both can be classified into three functional categories: inhibitory, activating and soluble secreted receptors. Members of the inhibitory receptors have 2 or 3 extra-cellular Ig-like domains in case of KIRs and 2 or 4 in case of LILRBs. They have a long cytoplasmic tail that has one or more immunoreceptor tyrosine-based inhibitory motif (ITIM). Members of the activating receptors have short cytoplasmic tail that has no ITIMs. They have a charged AA residue (arginine in the case of LILRAs) in the trans-membrane (TM) domain and they activate the cells by the association of this residue with an immunoreceptor tyrosine-based activation motif (ITAM)-bearing adaptor protein (like FcRγ, DAP12 and CD3ζ). The soluble secreted receptors retain the extra-cellular Ig-like domains and the signal peptide but lack the TM domain. The expression distribution of LRC genes is variable. While KIRs/KARs are expressed only in

natural killer (NK) cells and T cells, LILRs are expressed in lymphoid and myelomonocytic cells including T, B and NK cells, monocytes, macrophages and dendritic cells.[34,42] LAIRs are even broader in their expression range.[41]

Osteoclast-associated receptor (OSCAR) is one of the most recently identified members of the LRC genes.[43] Human OSCAR (hOSCAR) shows structural and functional similarities to the LILRAs. It has two extra-cellular Ig-like domains, arginine residue in the TM domain and a short cytoplasmic tail. It has been shown to associate with FcRγ and activates dendritic cells.[44] This shows that hOSCAR is a classical activating leukocyte receptor. hOSCAR expression has been reported in neutrophils, monocytes, macrophages and dendritic cells.[44]

While searching for genes differentially expressed during bone remodeling in a 7-day-old mouse calvaria using representational difference analysis (RDA), we isolated a novel cDNA clone that we initially called 3D10. A human EST clone that showed significant homology to the isolated clone was obtained and sequenced. 3D10 was found to be an alternatively spliced isoform of hOSCAR with substantially different C-terminus AA sequence. It has subsequently been named "OSCAR-S1" in the GenBank and registered by Kim et al (GenBank accession No. AF474152.1).[43] Human OSCAR gene is alternatively spliced into six isoforms. Careful analysis of these isoforms shows that only three have TM domains suggesting they are membrane receptors. The other three isoforms lack the TM domain but contain the signal peptide and the extra-cellular domain sequences present in the membrane receptor isoforms, which suggests they might be secreted isoforms.

Secreted receptors have been reported among LRC members (LILRA3 and LILRA5)[76] and other Ig-SF members (Mer receptor tyrosine kinase).[77] They represent a regulatory mechanism to the balance between receptors and their ligands.

OSCAR function has been reported to be important in inflammatory and immune response modulation and extends beyond the immune system to bone biology in osteoclast (OC) differentiation and function, a field named osteoimmunology.[52]

We have examined hOSCAR isoforms lacking the TM domain and compared the expression profiles with the membrane-bound hOSCAR isoforms. The soluble hOSCAR isoforms are novel isoforms that are secreted and may play an important role in hOSCAR regulation. To the best of our knowledge, these findings have not been reported or addressed in the previously published literature and they contribute to the understanding of osteo-immune biology and to the development therapeutic modalities to osteo-immune diseases.

Materials and Methods

Representational Difference Analysis (RDA) to isolate Differentially Expressed Genes

One week old mouse pups were used to obtain calvaria as the target tissue and their skin and tail as control/driver tissues. Following their sacrifice by quick decapitation, the calvaria were dissected out and all adherent soft tissues removed while keeping the pieces of calvaria in ice-cold PBS treated with DEPC. Skin and 1 cm tail samples were also dissected and collected separately. The tissues were immediately placed in tubes containing guanidine thiocyanate and homogenized. Total RNA was isolated using the guanidine thiocyanate-CsCl gradient method [47] and treated with RNase-free DNase. The quality of the RNA was determined by running small aliquots (15 μg) of each on formaldehyde-agarose gels.

Messenger RNA (mRNA) was isolated from 200 μg of total RNA from each of these tissues using Oligo dT magnetic beads (Novagen). The protocols for carrying out the RDA are described in detail elsewhere.[78] Differentially expressed cDNA fragments were cloned into the vector pSPORT-2. Randomly picked colonies were grown and plasmid DNA prepared using the Qiagen kit for minipreps. Forty one colonies were screened by sequencing and their cDNA sequence compared with entries in GenBank Sequence Database. Two novel clones were identified. One of them, termed 3D10 was used for further analysis. cDNA sequence showed homology to an EST clone that was obtained to assemble the full-length cDNA reading frame.

Sequence Analysis

Initially, the full length cDNA assembled from the human EST clone showed significant homology to the recently published human OSCAR except that there was no TM domain. Subsequent analysis revealed that OSCAR had several isoforms. Human OSCAR isoforms were aligned for nucleotide and AA sequences using Vector NTI 10.0.1 software (Invitrogen). Each protein sequence was analyzed for the presence of a TM domain by the following online programs: SOSUI system (http://bp.nuap.nagoya-u.ac.jp/sosui), TMHMM Server v. 2.0 (http://www.cbs.dtu.dk/services/TMHMM-2.0), TMpred (http://www.ch.embnet.org/software/TMPRED_form.html), and "DAS"-Trans-membrane Prediction server (http://mendel.imp.ac.at/sat/DAS/DAS.html); and for the presence of a signal peptide by SOSUIsignal (http://bp.nuap.nagoya-u.ac.jp/sosui/sosuisignal) and SignalP 3.0 Server (http://www.cbs.dtu.dk/services/SignalP).

Cell Lines

THP-1 cells (human myeloid monocytic cell line) were obtained from the American Type Culture Collection (ATCC, Manassas, VA). Cells were maintained at 37°C and 5% CO_2 in complete media composed of RPMI 1640 with 2 mM L-glutamine supplemented with 100 U/ml penicillin/streptomycin, non-essential AAs, 0.05 mM 2-mercaptoethanol (GIBCO Laboratories, Grand Island, NY), and 10% heat-inactivated fetal bovine serum (FBS) (Sigma-Aldrich, St. Louis, MO).

Phorbol Myristate Acetate (PMA) and Lipopolysaccharide (LPS) Stimulation

THP-1 cells were seeded in 6-well plates at the density of 10^6 cells/ml. PMA in DMSO or *E. coli* LPS (Sigma-Aldrich) were used to stimulate the cells with the following concentrations: 1, 10, 100 and 1000 ng/ml for 48 or 24 h, respectively. Adherent and suspended cells were processed for either RNA extraction or Western Blot analysis.

Semi-Quantitative RT-PCR

Total RNA from THP-1 cells was prepared using TRIzol Reagent (Invitrogen, Carlsbad, CA), and reverse transcribed using SuperScript II reverse transcriptase (Invitrogen). The Human 24 Tissue Rapid-Scan cDNA panel (OriGene Technologies, Inc., Rockville, MD), the Human Blood Fraction MTC Panel (Clontech Laboratories, Inc., Mountain View, CA) and Neutrophil cDNA (OriGene) were screened by Polymerase Chain Reaction (PCR) using specific primers for OSCAR: forward 5'-AGCTGCTGGTGACAGAGGAG-3', and reverse 5'-GTGTAGTCGGAGGAGCCAGA-3'. We used GAPDH primers for standardization and they were: forward 5'-ACCACAGTCCATGCCATCAC-3' and reverse 5'-

TCCACCACCCTGTTGCTGTA-3'. Expected PCR amplification product sizes are 833 bp for OSCAR isoforms with no TM domain, 319 bp for OSCAR isoforms with TM domain and 452 bp for GAPDH. PCR cycling conditions were 94°C for 3 min and 40 cycles of 94°C for 1 min, 51°C for 1 min, and 72°C for 2 min, and a final extension time of 72°C for 10 min, on a GeneAmp PCR System 9700 (Applied Biosystems, Foster City, CA). PCR products were run on 2% agarose gels. Intensity of the bands - Optical Density (OD) - was quantified by ImageJ software (National Institutes of Health, USA) and plotted using MS Office Excel (Microsoft Corporation, Costa Mesa, CA). For the Human 24 Tissue Rapid-Scan cDNA panel, GAPDH amplification was done using 100X panel and OSCAR amplification using the 1000X panel.

Analysis of Protein Expression by Western Blotting

THP-1 cells were stimulated with PMA as described before and cultured in serum-free media for 24 h. Culture media were collected and the cells washed with PBS before being lysed using RIPA buffer (50 mM Tris-HCl, 150 mM NaCl, 1% Triton X-100, 0.5% sodium deoxycholate, 0.1% SDS, and 1 mM EDTA, pH 7.4), containing 1X proteases inhibitor cocktail (Sigma). The collected conditioned media (CM) was concentrated 10-fold using Centriplus YM-10 centrifugal filter devices (Millipore, Bedford, MA). The concentrated CM was lyophilized overnight and re-suspended in dH_2O to give us samples that were concentrated approximately 100 folds. Aliquots of the concentrated CM were prepared and were either digested overnight using N-Glycanase (ProZyme, Inc., San Leandro, CA) or used as undigested samples. An aliquot of serum-free media was also digested as a negative control. Proteins in the cell lysates and media aliquots were separated by electrophoresis

using SDS-PAGE. Gels were transferred into nitrocellulose membranes and blotted. Western Blots were analyzed in duplicate using two separate antibodies that were raised in rabbits against synthetic peptides that were either common to all isoforms or specific to the isoform(s) with no TM domain. Antibody raised against the peptide RHSAQPWADFTLLGARAPG recognizes all isoforms of hOSCAR. A second rabbit polyclonal antibody raised against the C-terminus peptide QDSWDPAPPPSDPGV of our new hOSCAR isoform is specific to the isoform(s) that do not have the TM domain. Both the antibodies were made by Alpha Diagnostic Intl. Inc., San Antonio, TX. Mouse alpha-Tubulin antibody (DM1A) (Abcam, Cambridge, MA) was used as a loading control antibody for Western Blotting.

Results

hOSCAR has three pairs of membrane and soluble receptors

As of date, GenBank search for hOSCAR isoforms indicates the cDNA sequences of six isoforms with the following accession numbers; OSCAR1 (NM_206818.1), OSCAR3 (NM_130771.2), OSCAR4 (NM_133169.2), OSCAR5 (NM_133168.2), OSCAR-S1 (AF474152.1), and OSCAR-S2 (AF474153.1). They were all registered by Kim et al.[43] Human OSCAR gene consists of six exons. Alternative splicing process results in six variants. Aligning their nucleotide sequences shows that three of them have an unspliced intron between exon V and VI (Figure 4.1 A). This unspliced intron is approximately 500 bp long, which results in the presence of three long and three short cDNA sequences. Mouse OSCAR (mOSCAR) gene consists of five exons and the unspliced intron does not exist in the currently identified three alternatively spliced isoforms. There is one short, and two long

transcripts with a difference of approximately 600 bps at the 3' un-translated region of the last exon (Data not shown).

AA sequences of proteins encoded by hOSCAR cDNA isoforms show six different isoforms (Figure 4.1 B). Analyzing the splicing pattern shows that there are three pairs of proteins. Each pair consists of an identical N-terminus polypeptide sequence but one molecule with and one without a TM domain at the C-terminus end in each pair. This is caused by the presence of a stop codon within the unspliced intron preventing exon VI from being translated, which carries the TM domain encoding sequence. Isoforms lacking the TM domain are only 19 AA-longer than their counterparts. This is because the translated region from the unspliced intron is longer than the one from exon VI. To avoid confusion between the various isoforms, we are proposing a new nomenclature for hOSCAR isoforms as shown in Table 4.1. Basically, isoforms with no TM domains in their AA sequence (soluble isoforms) will be abbreviated hOSCARs 1-3 and those with a TM domain in their C-terminal end (membrane-bound, receptor) abbreviated as hOSCARm 1-3. As per the proposed new nomenclature, the longest pair is OSCARs1 and OSCARm1. OSCARs2 and OSCARm2 have exon III spliced out, and OSCARs3 and OSCARm3 have both exon II and III spliced out. All isoforms have predicted signal peptides. The N-terminus of all isoforms (the extra-cellular domain of the membrane receptors) has two Ig-like domains each one is encoded by a different exon.

The three isoforms of mOSCAR encode only two proteins (two transcripts with identical coding regions but different 3' untranslated regions and one transcript that is slightly shorter). The difference in the AA sequence between the two protein isoforms is at the N-terminus with 6 AAs (one exon) missing in the shorter isoform (data not shown).

hOSCAR is differentially expressed in many tissues

Since the soluble form of hOSCAR (hOSCARs) is a novel finding, we investigated its mRNA distribution in a human tissue cDNA panel and compared it to the distribution of the membrane receptor hOSCAR mRNA (hOSCARm) using RT-PCR. Primers were designed to amplify both groups in the same PCR reaction with the difference of amplicon size taking advantage of the unspliced intron specificity to the soluble isoforms. Figure 4.2 A. shows that both forms are differentially expressed in most tissues screened. The intensity of the band for membrane receptor isoforms was stronger in general. The intensity of the PCR amplified bands was normalized to the GAPDH mRNA levels (Figure 4.2 B) and the findings reveal that the abundance of the two groups is not equally distributed nor has similar distribution pattern among tissues.

hOSCAR is differentially expressed in all mononuclear cells and is down-regulated by lectin mitogen activators

It has been reported that hOSCAR is expressed in myeloid cells.[44] We investigated the expression of both groups of hOSCAR in a cDNA panel and found that both groups are actually expressed abundantly in all mononuclear cells screened (Figure 4.3). While both groups are down-regulated by lectin mitogen activators (PHA, Con A and PWM), hOSCARm is almost abolished in unsorted MNC and in both T- and B-cells.

PMA and LPS-stimulated THP-1 cells over-express hOSCAR mRNA

We selected the THP-1 human monocytic cell line to screen the mRNA expression of the two groups of hOSCAR. Un-stimulated THP-1 cells were found to express both isoform groups at a basal level (Figure 4.4). Macrophage induction with PMA results in over-expression of the hOSCARs isoforms in a dose response manner, while the level of the hOSCARm isoforms does not change. LPS activation showed a similar pattern but the over-expression did not change with increasing the dose above 1 ng/ml. Adding PMA first followed by LPS showed no difference compared to each stimulant individually.

At the protein level, lysates from both un-stimulated and stimulated THP-1 cells showed a band of approximately 29-30 kDa that did not change in intensity with the different treatments when screened using the hOSCAR antibody that recognizes all isoforms (Figure 4.5). This band size corresponds to the calculated size of both hOSCAR isoform groups (Table 4.1).

Soluble hOSCAR isoform is secreted

To investigate whether the new hOSCARs isoform that has signal peptide is secreted, we examined the conditioned media from PMA-stimulated THP-1 cells. The approximately 100-folds concentrated media showed a band of approximately 29-30 kDa. Next we examined the possibility of glycosylation of the secreted isoform by digesting the protein with N-Glycanase before analyzing by Western Blotting. The results using both the polyclonal antibodies are shown in figure 4.6. Ab specific to the soluble isoforms also showed a faint wide band at approximately 45 kDa in the undigested media, suggesting the possible presence of glycosylated forms.

Discussion

Human OSCAR gene maps to LRC on chromosome 19q13.42. This cluster has been receiving more interest lately due to new members added, old members characterized and differences between species studied. Currently, only OSCAR and NKp46 have orthologs in human and rodents.[79,80] Interestingly, NKp46 was suggested to be the boundary of LRC on one end in both human and mouse and LILRB3 and the PIR family in human and mouse respectively [81] but now NKp46 and OSCAR represent LRC boundaries. More members might be added in the future due to the complexity and new understanding of this cluster. There are some differences between hOSCAR and mOSCAR and several similarities between hOSCAR and other members of LRC. The mOSCAR has been shown to be Osteoclast-specific and is expressed only in committed pre-Osteoclasts [43] while hOSCAR has been shown to be expressed in several MNC of myeloid origin [44] which suggests a need for tighter regulatory mechanism of its function. One of the very important regulatory mechanisms that exist in LRC members, like the LILRs, is alternative splicing and production of soluble receptors.[76] Soluble receptors provide a mechanism to regulate the balance between receptors and their ligands.

In this study we identified a spliced isoform of hOSCAR that is soluble and secreted into the extra-cellular compartment. We have also suggested a revised nomenclature of the different isoforms of hOSCAR comparing their splicing pattern and AA sequences for better understanding of this family of proteins and avoiding confusion. We have shown how the presence of the stop codon in the unspliced intron prevents the translation of the TM domain yet the extra-cellular domain is completely translated and theoretically can bind, presumably

to the same ligand. Whether the differences in the N-termini of the extra-cellular domain between different isoforms affect ligand binding specificity and/or efficiency is not known at present. Alternatively, such minor differences may have no functional relevance. It was interesting to find that each membrane receptor isoform has a partner that is soluble with almost identical AA sequence. This supports the notion that structural difference may have functional effects. The soluble isoforms have a relatively longer C-terminal domain. Whether the extra AA sequences in the C-terminal ends of soluble isoforms serve direct functions or affect the folding of these soluble isoforms is not known. Similarly, the transcriptional regulation of all these different isoforms has yet to be studied.

The existence of the soluble isoforms led us to investigate their expression distribution and compare them to the membrane receptor isoforms. Designing specific primers for soluble isoforms as a group was easy due to the presence of the intron but specific primers for individual isoforms of either group or the membrane receptor group was only possible across the splicing regions. In this study we used a common set of primers specific for hOSCAR but can detect both groups in the same reaction and the difference would be in the amplicon size. Both groups were found in lymphoid and almost all other tissues but with differences in the intensity of the PCR bands within and between the groups. This indicates that transcriptional regulation is tissue-specific depending on the cell type expressing OSCAR. mRNA expression distribution in leukocytes showed that both groups are highly expressed in all resting MNC including T- and B-cells. This contradicts finding by Merck et al.[44] and could be possibly explained by two factors: the quality of cDNA from T- and B-cells could have been different (housekeeping gene expression control), and primers used could not detect OSCARs3 and OSCARm3. An interesting finding is that all

lectin mitogen activators used show down-regulation of both groups and almost abolished the membrane-bound group. These mitogens increase IL-2 production which is nuclear factor of activated T cells (NFAT) transcription factor-dependent.[82] Although NFAT activity is increased, which up-regulates mOSCAR,[83,84] other transcription factors could be severely suppressed like microphthalmia transcription factor (MITF) in activated B-cells.[85] A complete transcriptional regulation of OSCAR is not fully studied especially in human. Our findings will assist in this field. The down-regulation of hOSCAR isoforms could suggest a low functional importance in these cells post-activation. Although MNC collectively showed the same effect of down-regulation, CD14+ monocytes were not activated separately by mitogens. It would be interesting to find out the effect on these cells since PMA and LPS showed the opposite effect on THP-1 cells which are monocytic cell line. PMA induces THP-1 cells to differentiate into macrophages morphologically and functionally through protein kinase C (PKC) pathway.[86] PKC is known to activate NFAT [87,88] which might explain the up-regulation of hOSCAR soluble isoforms. This effect was not observed in the membrane receptors. A transcriptional difference is a possible explanation. LPS activation showed similar up-regulation level for soluble hOSCAR isoforms with the lowest dose but no additive or synergistic effect was observed after PMA stimulation. Our findings were in agreement with what has been reported of LPS neutral effect on membrane hOSCAR isoforms.[89] We did not detect any expression difference between stimulated and non-stimulated THP-1 cell lysates at the protein level. This could be because the molecular mass of the two groups overlaps within a small range. There is a possibility that membrane receptors band masked the soluble receptors band.

The hypothesis that the soluble hOSCAR isoforms are secreted has been confirmed by western blot of conditioned media from PMA-stimulated THP-1 cells. This finding provides an additional difference between mOSCAR and hOSCAR and a similarity to some other LRC members. Secreted receptors are formed by alternative splicing or proteolytic cleavage.[90] These two mechanisms could exist together in one gene as in the case of IL-4 and IL-6 receptors. It would not be surprising to find out that membrane-bound hOSCAR could be released by proteolytic cleavage. Secreted receptors sequester ligands and/or eliminate the membrane receptor in the case of proteolytic cleavage. They play an important role in the pathophysiology of immune and bone diseases by altering the balance between activation and inhibition. They have been also used for therapeutic purposes to facilitate treatment and monitoring disease processes.[90] These secreted hOSCAR isoforms might provide an alternative mechanism to an ITIM receptor binding the same ligand as in the case of several LRC members with known MHC class I ligands.[91] The ligand of hOSCAR has not been identified yet but a putative ligand for mOSCAR has been detected on osteoblasts.[43]

In conclusion, we identified a new group of hOSCAR that is secreted and may act as decoy receptors to regulate hOSCAR function keeping the balance between the activating nature of hOSCAR and the inhibition needed to prevent excessive immune response and bone destruction. Identifying hOSCAR ligand and evaluating receptor/ligand expression biologically and in osteo-immune diseases will help further elucidate hOSCAR function and therapeutic potential.

Tables

Table 4.1. Suggested New Nomenclature of hOSCAR Isoforms and their Characteristics.

Isoform		Group/Protein Nature	cDNA Size (bp)	Polypeptide Length (AA)	Molecular Weight (kDa)
Current Name	***Suggested New Name***				
OSCAR1	**hOSCARs1**	Soluble/Secreted	1946	286	30.9
OSCAR-S1	**hOSCARs2**	Soluble/Secreted	1897	282	30.5
OSCAR-S2	**hOSCARs3**	Soluble/Secreted	1826	271	29.2
OSCAR3	**hOSCARm1**	Membrane-Bound	1440	267	29.2
OSCAR4	**hOSCARm2**	Membrane-Bound	1428	263	28.8
OSCAR5	**hOSCARm3**	Membrane-Bound	1395	252	27.6

Figure Legends

Figure 4.1. Human OSCAR isoforms sequence comparison.

(A) A schematic illustration drawn to scale for hOSCAR gene showing exon/intron organization of the longest isoforms hOSCARs1 and hOSCARm1 with a parallel encoded polypeptide sequences and their main domains. Human OSCAR gene consists of six exons and one unspliced intron between exon V and VI. Due to the presence of a stop codon in the unspliced intron, the resulting protein lacks the TM domain that is present when the intron is spliced out. There is a signal peptide at the N-terminus region of all the spliced forms predicted to be 18 AA-long. All isoforms have 2 Ig-like domains each one is encoded by a separate exon. Numbers represent AA residues. (B) AA sequence alignment of hOSCAR isoforms. Alternative splicing process to exons II and III and the unspliced intron results in six variants; three with and three without the TM domain. Isoforms lacking the TM domain are 19 AAs longer than their counterparts.

Figure 4.2. PCR of human tissue cDNA panel.

(A) A 2% agarose gel electrophoresis of PCR products shows a relative distribution of hOSCAR groups in 24 different human tissues. (B) Normalized OD to GAPDH mRNA expression shows that both forms are expressed in almost all tissues. The abundance of the two groups is not equally distributed nor has similar distribution pattern among tissues.

Figure 4.3. PCR of blood cells cDNA panel.

(A) A 2% agarose gel electrophoresis of PCR products of a Clontech cDNA panel of resting and activated T-, B- and mononuclear cells (MNC) and resting monocytes (MO), and an

OriGene cDNA of Neutrophils shows a relative distribution of hOSCAR groups mRNA expression. According to the supplier, activation was done as follows: CD8+ cells by 5 µg/ml phytohemagglutinin (PHA) for 3 days, CD4+ cells by 5 µg/ml concanavalin A (Con A) for 3-4 days, CD19+ cells by 2 µ/ml pokeweed mitogen (PWM) for 4 days, and MNC by 2 µl/ml PWM and 5 µg/ml Con A for 3 days. (B) After normalizing the OD to GAPDH levels, mRNA expression shows that both forms are down-regulated by the lectin mitogen activators.

Figure 4.4. RT-PCR of PMA/LPS-stimulated THP-1 cells.

(A) A 2% agarose gel electrophoresis of PCR products of cDNA of THP-1 cells stimulated by PMA and LPS (dose as indicated). (B) After normalizing the OD to GAPDH levels, mRNA expression relative to the non-stimulated cells shows that there is a clear dose-response up-regulation of hOSCARs group with PMA stimulation. LPS shows some up-regulation as well but without dose-response. (C) hOSCARm group expression is not significantly altered.

Figure 4.5. Western blot of PMA/LPS-stimulated THP-1 Cells.

THP-1 cells were stimulated with PMA and LPS as indicated. The cells were harvested and the lysates were analyzed by Western blot using anti-hOSCAR and anti-α-Tubulin, antibodies. Human OSCAR bands are approximately 29-30 kDa, corresponding to their calculated size. There is no change in the expression level between the stimulated versus the non-stimulated cells.

Figure 4.6. Soluble receptor hOSCAR isoforms are secreted.

Western blot analysis using anti-hOSCAR Ab (A) and anti-hOSCARs Ab (B) show that the soluble receptor hOSCARs isoforms are present in the N-Glycanase-digested (D) and undigested (UD) conditioned media (CM) of THP-1 cells. Digested serum-free (SF) media was used as a negative control. A wide band of approximately 45 kDa appears in the undigested media in the blot with anti-soluble hOSCAR Ab representing the glycosylated isoforms.

Figures

Figure 4.1

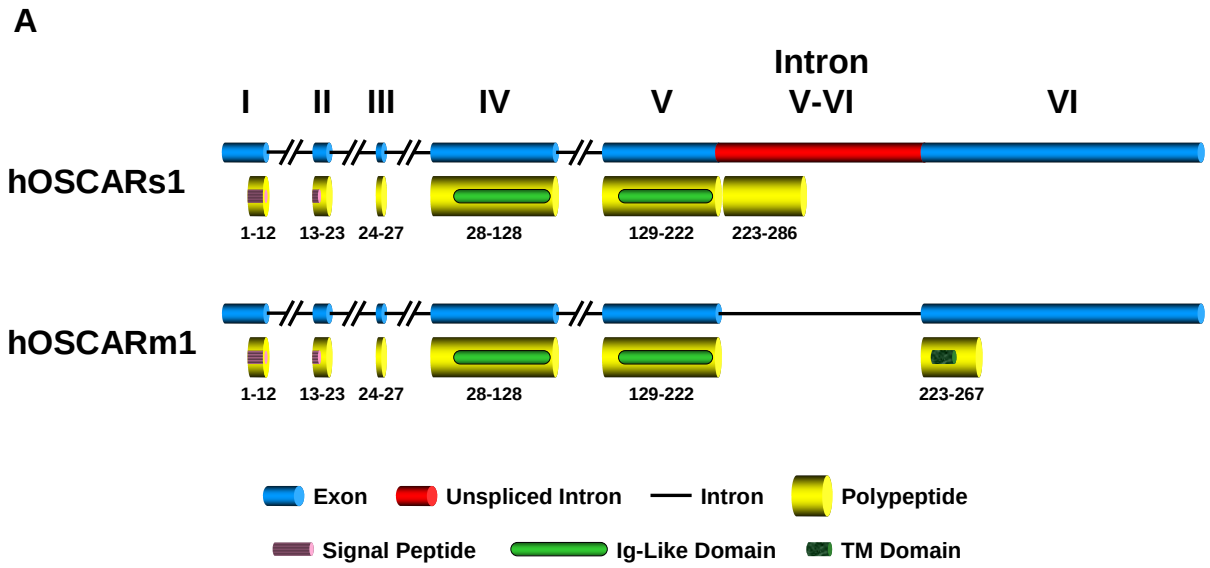

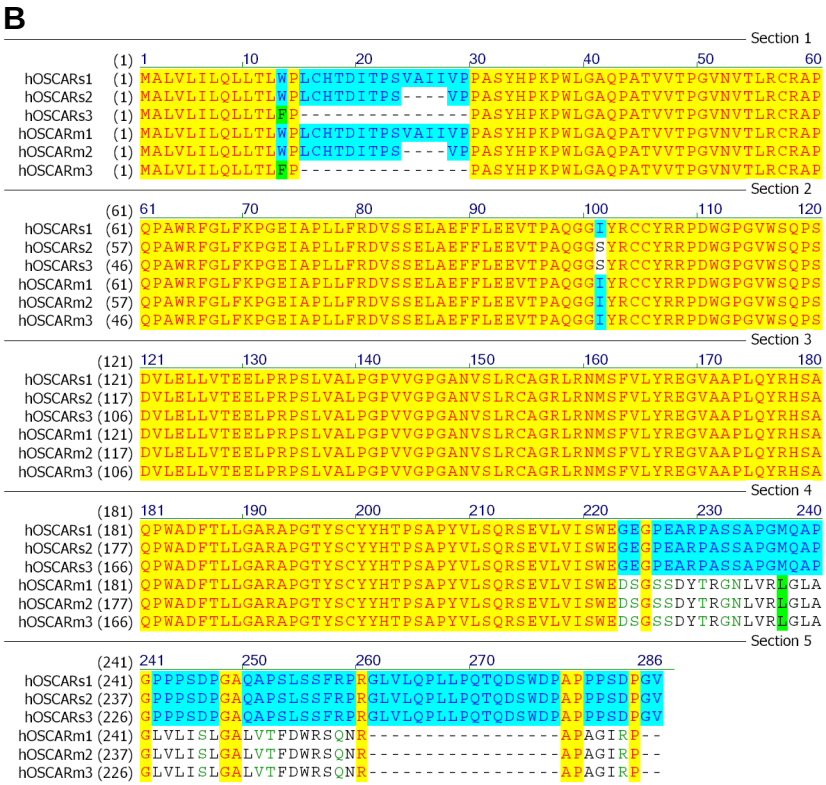

Figure 4.2

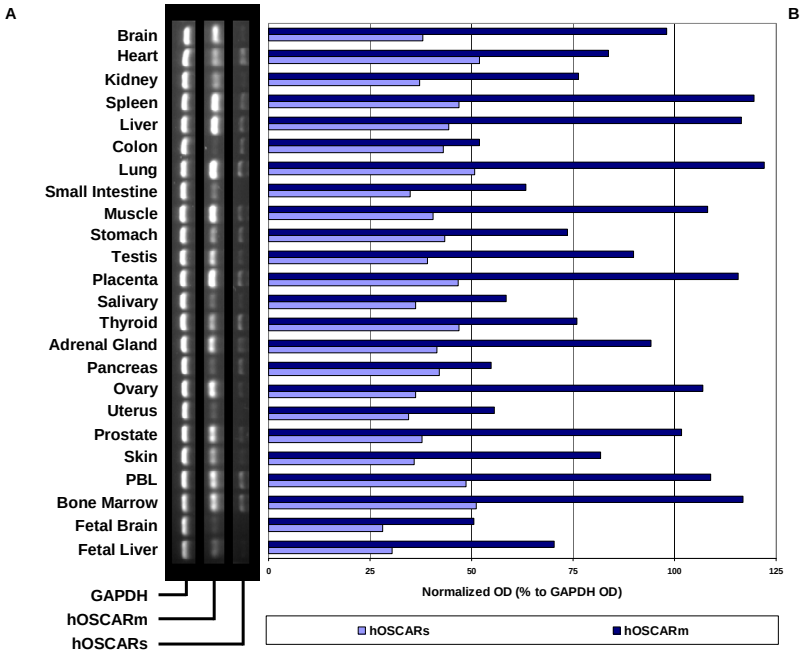

Figure 4.3

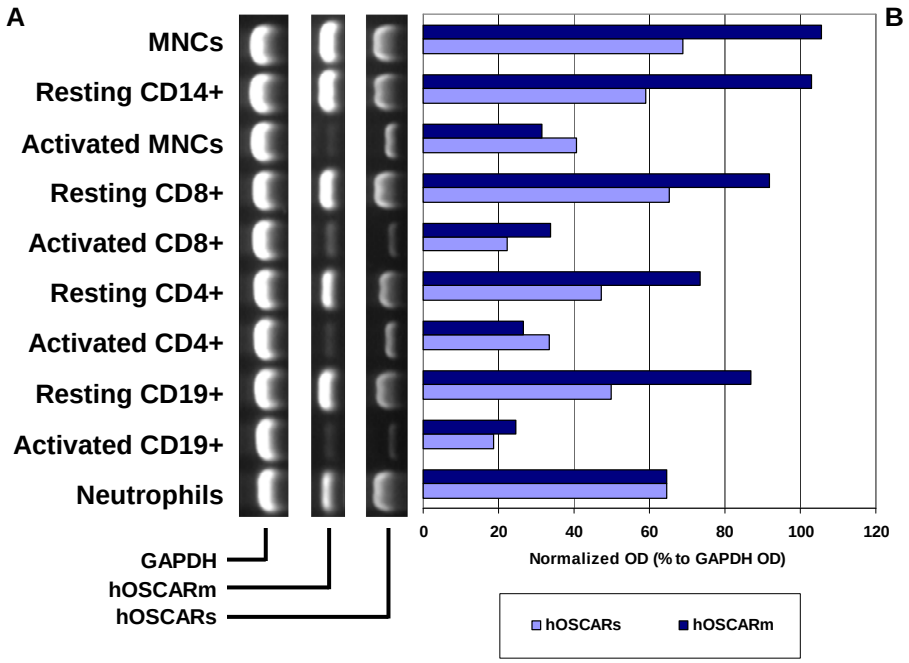

Figure 4.4

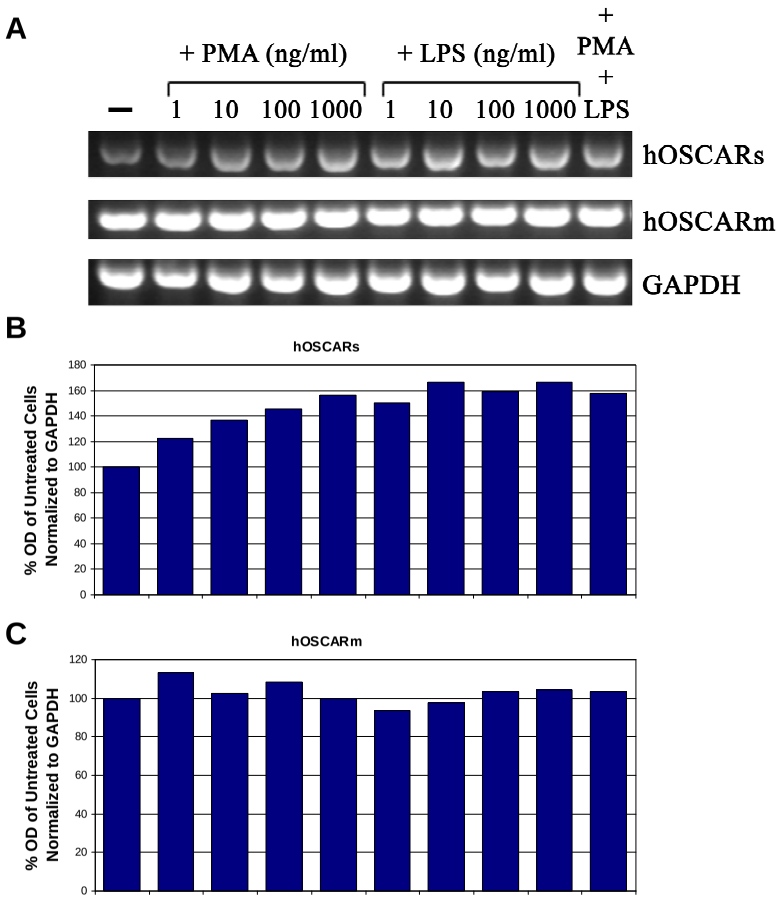

Figure 4.5

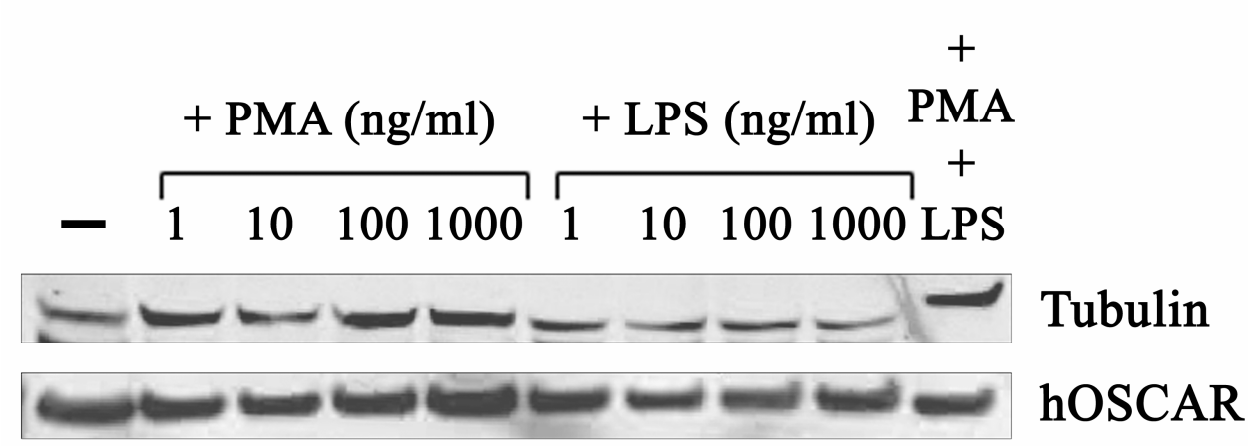

Figure 4.6

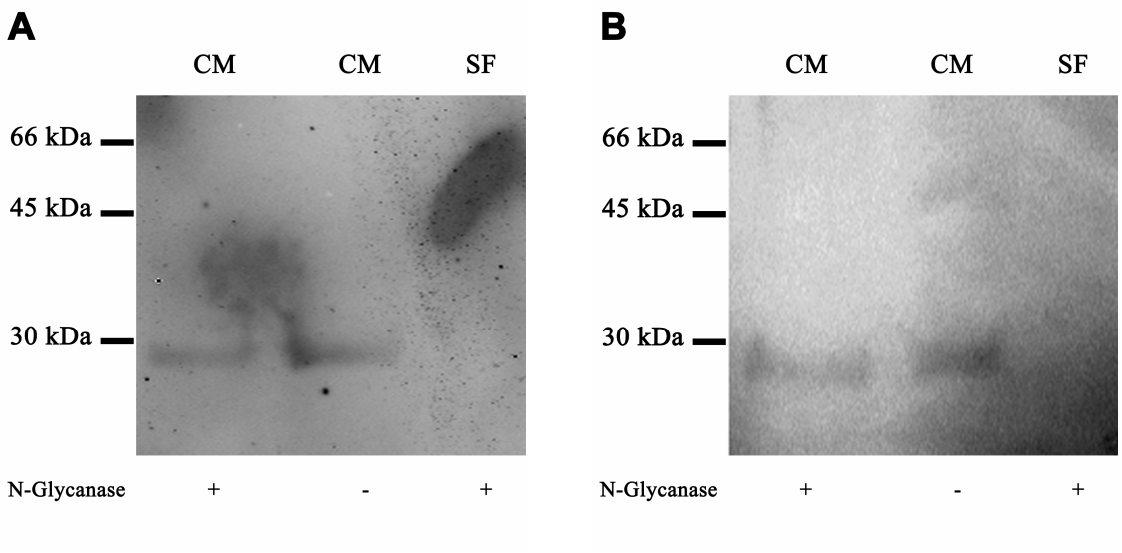
A
CM
CM
SF
66 kDa
45 kDa
30 kDa
N-Glycanase
+
-
+
B
CM
CM
SF
66 kDa
45 kDa
30 kDa
N-Glycanase
+
-
+

DISCUSSION & CONCLUSIONS

OSCAR was discovered in mouse and thought to be OC-specific gene.[43] We isolated OSCAR fragment from mouse calvaria which shows the importance of this gene during bone development. Mouse OSCAR has been shown to play an important role as a co-stimulatory signaling receptor cooperating with RANK for OC differentiation.[92] We have shown that in human OSCAR is widely expressed in many tissues including bone marrow, lymphoid and non-lymphoid tissues. This suggests a broader function of OSCAR in human depending on the type of tissue and the cells expressing it. hOSCAR is expressed in the myeloid cells DC, MO and MΦ, in addition to OC.[50] We have shown that hOSCAR is also expressed in T and B lymphocytes. hOSCAR has been shown to be important in maturation, activation, survival and antigen presentation of DC.[74] It has also been shown to enhance the pro-inflammatory response of neutrophils and MO.[89] Since hOSCAR is an activating receptor, its expression in T cells suggests an activating function especially that the only LILR gene that is expressed on T cells is LILRB1 which is an inhibitory receptor.[93] Similarly, hOSCAR's expression in B cells represents a regulatory mechanism to the inhibitory receptors. PIR-A which is a mouse activating receptor similar to LILRA receptors, counteracts the inhibitory effect of PIR-B on B cells.[94,95] The secreted hOSCAR isoforms themselves represent a regulatory mechanism to hOSCAR receptor function and activation especially if they are expressed by the same cell. The finding that both groups of hOSCAR are down-regulated by lectin mitogen activators in lymphocytes was very interesting. Lectin mitogens could down-

regulate hOSCAR due to an opposing pathway to the activation through hOSCAR stimulation. This is supported by the observation of the significant diminishing of the membrane-bound isoforms compared to the secreted isoforms. The down-regulation could be direct transcriptional regulation or indirect through another pathway or molecule. There is a possibility that the down-regulation is a feedback inhibition through hOSCAR activation. These mitogen activators could bind hOSCAR and activate the receptor followed by hOSCAR self-regulation. The expression profile during the activation process, which took 3-5 days, was not possible to study. The wide expression of hOSCAR in immune cells indicates its involvement in both the innate and adaptive immunity. Other cell surface receptors that share very similar structural and functional features with hOSCAR are members of the LILR family within the LRC. hOSCAR gene maps to chromosome 19q13.42, where other genes of LRC are located. Families of genes within this cluster have no true orthologs in human and rodents except OSCAR and NKp46. The PIR family in mouse resembles the LILR family in human in terms of their sequence, expression pattern, ligands, signaling, and function. Alternative splicing is a common feature found in these genes which results in different isoforms some of which have no TM domain and could be secreted. Secreted members of LRC in human include LILRA3,[34] LILRA5,[76] and LILRB2 [96] from the LILR family, LAIR2 [41] from the LAIR family, and KIR3DP1 [97] from the KIR family. We have added one more member to this list which is hOSCAR with its 3 isoforms. In mouse LRC, there has been no identified soluble (secreted) receptor. We have shown evidence suggests the existence of soluble form of mOSCAR using the rabbit anti-soluble hOSCAR Ab. If this is confirmed by sequencing the band recognized by this Ab, OSCAR will become the first soluble member of mouse LRC. Secreted receptors play important role

in regulating the balance between receptor-ligand binding and the consequent activation or inhibition of that receptor. We have presented a group of 3 different isoforms of soluble hOSCAR and confirmed the expression and secretion of this form. We have shown that these 3 isoforms along with the 3 membrane-bound isoforms form 3 pairs. The difference between these pairs is in the extra-cellular domain. These differences suggest functional differences in ligand binding specificity and/or efficiency as in the example of LILRB2 which shares 82% identity with LILRB1 extra-cellular domain but it binds its ligand with 1500-fold lower affinity.[98] The ligand for hOSCAR has not been identified but evidence suggest that it is expressed on the surface of osteoblast. Many members of LRC are of unknown ligand. LILR family has been divided into 2 groups based on sequence alignment and homology to LILRB1.[99] Group 1 was suggested to bind MHC I molecules based on known findings of at least 3 members [100] and the comparison between the known crystal structures and the AA residues of MHC I binding site.[91] This comparison suggested that members of group 2 do not play a role in any MHC I recognition. Other members of LRC have been reported to bind MHC I and non-MHC I. Some KIR members bind MHC I, GPVI binds collagen, LAIR binds epithelial cellular adhesion molecule, FcαR binds IgA, and gp49B binds integrin $\alpha_v\beta_3$.[100] Among the list of the yeast two hybrid screening results there are some strong candidates like MHC I molecules and some membrane proteins that could be the ligand(s) for hOSCAR. Others could be intra-cellular modulators especially when we consider the inhibition of NF-κB observed by the over-expression of cloned 3D10. Some of these candidates are currently under investigation. Identifying and characterizing hOSCAR ligand(s) would clearly lead to better understanding of this important receptor function and potential. Its ligand(s) could also be the same for other receptors of LRC.

To date, what is known about the expression modulation and transcriptional regulation of hOSCAR is very little. Most of the current studies have been focused on mOSCAR. mOSCAR has been shown to be regulated by microphthalmia transcription factor (MITF), PU.1 [101] and NFATc1.[83,84,102] Unfortunately, MITF and PU.1 sites present in mOSCAR promoter are not present in hOSCAR promoter.[50] mOSCAR has been reported to be inhibited by the over-expression of MafB/Kreisler [103] and Protein inhibitor of activated STAT3 (PIAS3).[102] Some LILR members have been found to be regulated by Sp1, chromatin modifications and histone acetylation, PU.1, Runx1, and CMV infection.[104] Whether hOSCAR shares some of these regulators or not is not known at present. Membrane-bound hOSCAR was found to be inhibited by LILRB1.[105] Its level was not found to be altered by LPS, Pam3Cys (synthetic palmitoylated mimic of bacterial lipopeptides), R-848 (imidazoquinoline resiquimod), or GM-CSF in neutrophil or MO.[89] However, we have shown that the secreted hOSCAR is up-regulated by LPS and PMA in MO. During activation of MO, inflammatory response needs to be controlled and regulated to prevent the over-activation. In addition, the enhanced inflammatory response of MO to suboptimal dose of LPS when hOSCAR is stimulated could be damaging to the tissues.[89] This explains why the secreted isoforms are up-regulated by LPS. They could also be involved in sequestering the ligand to prevent another pathway of MO differentiation to OC. This is supported by the finding that these isoforms are also over-expressed during MO differentiation into MΦ by PMA stimulation. It would be interesting to investigate the expression profile of all these isoforms in OC during the different stages of differentiation and activation. It appears that the secreted hOSCAR isoforms in MO favors the immune response over OC differentiation

but prevent the over-activation and the enhanced survival of MΦ caused by the membrane-bound isoforms in the presence of LPS.

Although the soluble hOSCAR isoforms are secreted, they could be expressed and remain intra-cellular. It has been reported that all CD4+ and CD8+ clones may be positive for intra-cellular LILRB1 irrespective of the surface expression of this receptor.[93] We observed the inhibition of over-expressed 3D10 to NF-κB which could be specific or general to other transcription factors that are important in the inflammatory response. This further confirms the opposite role of the two groups of hOSCAR since the soluble isoforms inhibit NF-κB and the membrane-bound isoforms enhance the inflammatory response and also osteoclastogenesis which is NF-κB-dependant.

The future of hOSCAR research looks very demanding. Clinically, OSCAR promoter polymorphism has been associated with bone mineral density (BMD) in postmenopausal women.[106] Several clinical studies have been conducted to link some of LRC gene families to diseases failed to identify the gene of interest. Coeliac disease and systemic lupus erythematosus (SLE) has been linked to LRC region,[107,108] and psoriasis vulgaris is associated with MHC class I.[109] hOSCAR could be that unknown gene. Studying OSCAR will face some problems because there has been no reported animal model. Since mOSCAR is not expressed in immune cells, it is impossible to evaluate the interaction between the different biological processes involving OSCAR in mouse and correlate it with human. One of the solutions is a transgenic mouse. Transgenic mice have been generated for LILR and KIR genes since these families have either no true homolog or do not exist at all.[110]

In conclusion, we isolated a novel protein that we named 3D10. It is one of six alternatively spliced isoforms of hOSCAR. We showed that hOSCAR is expressed in both membrane-bound and soluble isoforms. Each membrane-bound isoform has and identical soluble one making three pairs. Each pair shares a slight different extra-cellular (N-terminus) domain that suggests functional differences. Although mOSCAR gene does not have soluble isoforms identified, we showed some evidence supports their existence. The confirmation is pending sequencing the band identified by anti-3D10 Ab in mouse tissues and RAW 264.7 cells. We presented that hOSCAR isoforms are widely expressed in human tissues and MNC including T- and B-lymphocytes. We also showed that PMA and LPS increase the expression of the soluble isoforms and lectin mitogen activators down-regulate all isoforms but have more effect on the membrane-bound isoforms. OSCAR ligand has not been identified but we presented a list of potential ligand(s) and binding partners by the yeast-two-hybrid screening. Some of these proteins are currently under investigation. We confirmed that the soluble isoforms of hOSCAR are actually secreted. Given the structural properties, their function is suggested to be as decoy receptors regulating OSCAR activation by ligand binding. Finally, although 3D10 has been found to be secreted, over-expressed intra-cellular 3D10 inhibits NF-κB in a TNF-α-independent pathway. These findings expand our knowledge about receptors regulating the osteoimmunology and present a potential for better understanding of human biology which will lead to better therapeutic modalities and health.

BIBLIOGRAPHY

1. van Furth R, Cohn ZA, Hirsch JG, Humphrey JH, Spector WG, Langevoort HL. The mononuclear phagocyte system: a new classification of macrophages, monocytes, and their precursor cells. Bull World Health Organ. 1972;46:845-852.

2. Miyamoto T, Ohneda O, Arai F, et al. Bifurcation of osteoclasts and dendritic cells from common progenitors. Blood. 2001;98:2544-2554.

3. Naito M. Macrophage heterogeneity in development and differentiation. Arch Histol Cytol. 1993;56:331-351.

4. Stanley ER, Berg KL, Einstein DB, et al. Biology and action of colony--stimulating factor-1. Mol Reprod Dev. 1997;46:4-10.

5. Zaidi M, Blair HC, Moonga BS, Abe E, Huang CL. Osteoclastogenesis, bone resorption, and osteoclast-based therapeutics. J Bone Miner Res. 2003;18:599-609.

6. Karin M, Yamamoto Y, Wang QM. The IKK NF-kappa B system: a treasure trove for drug development. Nat Rev Drug Discov. 2004;3:17-26.

7. Kracht M, Saklatvala J. Transcriptional and post-transcriptional control of gene expression in inflammation. Cytokine. 2002;20:91-106.

8. Fujihara M, Muroi M, Tanamoto K-i, Suzuki T, Azuma H, Ikeda H. Molecular mechanisms of macrophage activation and deactivation by lipopolysaccharide: roles of the receptor complex. Pharmacology & Therapeutics. 2003;100:171-194.

9. Roodman G. Advances in bone biology: the osteoclast. Endocr Rev. 1996;17:308-332.

10. Teitelbaum SL, Ross FP. Genetic regulation of osteoclast development and function. Nat Rev Genet. 2003;4:638-649.

11. Katagiri T, Takahashi N. Regulatory mechanisms of osteoblast and osteoclast differentiation. Oral Dis. 2002;8:147-159.

12. Yasuda H, Shima N, Nakagawa N, et al. Osteoclast differentiation factor is a ligand for osteoprotegerin/osteoclastogenesis-inhibitory factor and is identical to TRANCE/RANKL. Proc Natl Acad Sci U S A. 1998;95:3597-3602.

13. Tsuda E, Goto M, Mochizuki S-i, et al. Isolation of a Novel Cytokine from Human Fibroblasts That Specifically Inhibits Osteoclastogenesis*1, *2. Biochemical and Biophysical Research Communications. 1997;234:137-142.

14. Udagawa N, Takahashi N, Akatsu T, et al. Origin of Osteoclasts: Mature Monocytes and Macrophages are Capable of Differentiating Into Osteoclasts Under a Suitable Microenvironment Prepared by Bone Marrow-Derived Stromal Cells. PNAS. 1990;87:7260-7264.

15. Khapli SM, Mangashetti LS, Yogesha SD, Wani MR. IL-3 acts directly on osteoclast precursors and irreversibly inhibits receptor activator of NF-kappa B ligand-induced osteoclast differentiation by diverting the cells to macrophage lineage. J Immunol. 2003;171:142-151.

16. Baqui AAMA, Meiller TF, Chon JJ, Turng B-F, Falkler WA, Jr. Granulocyte-Macrophage Colony-Stimulating Factor Amplification of Interleukin-1beta and Tumor Necrosis Factor Alpha Production in THP-1 Human Monocytic Cells Stimulated with Lipopolysaccharide of Oral Microorganisms. Clin Diagn Lab Immunol. 1998;5:341-347.

17. Weil MH, Shubin H, Biddle M. Shock Caused by Gram-Negative Microorganisms.Analysis of 169 Cases. Ann Intern Med. 1964;60:384-400.

18. Galanos C, Freudenberg MA. Mechanisms of endotoxin shock and endotoxin hypersensitivity. Immunobiology. 1993;187:346-356.

19. Morrison DC, Ryan JL. Endotoxins and disease mechanisms. Annu Rev Med. 1987;38:417-432.

20. Wright SD, Ramos RA, Tobias PS, Ulevitch RJ, Mathison JC. CD14, a receptor for complexes of lipopolysaccharide (LPS) and LPS binding protein. Science. 1990;249:1431-1433.

21. Yang H, Young DW, Gusovsky F, Chow JC. Cellular events mediated by lipopolysaccharide-stimulated toll-like receptor 4. MD-2 is required for activation of mitogen-activated protein kinases and Elk-1. J Biol Chem. 2000;275:20861-20866.

22. O'Neill LA, Dinarello CA. The IL-1 receptor/toll-like receptor superfamily: crucial receptors for inflammation and host defense. Immunol Today. 2000;21:206-209.

23. Hume DA, Ross IL, Himes SR, Sasmono RT, Wells CA, Ravasi T. The mononuclear phagocyte system revisited. J Leukoc Biol. 2002;72:621-627.

24. Itoh K, Udagawa N, Kobayashi K, et al. Lipopolysaccharide promotes the survival of osteoclasts via Toll-like receptor 4, but cytokine production of osteoclasts in response to lipopolysaccharide is different from that of macrophages. J Immunol. 2003;170:3688-3695.

25. Takami M, Kim N, Rho J, Choi Y. Stimulation by toll-like receptors inhibits osteoclast differentiation. J Immunol. 2002;169:1516-1523.

26. Zou W, Bar-Shavit Z. Dual modulation of osteoclast differentiation by lipopolysaccharide. J Bone Miner Res. 2002;17:1211-1218.

27. Xie J, Qian J, Wang S, Freeman ME, III, Epstein J, Yi Q. Novel and Detrimental Effects of Lipopolysaccharide on In Vitro Generation of Immature Dendritic Cells: Involvement of Mitogen-Activated Protein Kinase p38 J Immunol. 2003;171:4792-4800.

28. Ziegler-Heitbrock HW, Frankenberger M, Wedel A. Tolerance to lipopolysaccharide in human blood monocytes. Immunobiology. 1995;193:217-223.

29. Ziegler-Heitbrock HW. Molecular mechanism in tolerance to lipopolysaccharide. J Inflamm. 1995;45:13-26.

30. Wende H, Colonna M, Ziegler A, Volz A. Organization of the leukocyte receptor cluster (LRC) on human chromosome 19q13.4. Mamm Genome. 1999;10:154-160.

31. Wagtmann N, Biassoni R, Cantoni C, et al. Molecular clones of the p58 NK cell receptor reveal immunoglobulin-related molecules with diversity in both the extra- and intracellular domains. Immunity. 1995;2:439-449.

32. Vivier E, Daeron M. Immunoreceptor tyrosine-based inhibition motifs. Immunol Today. 1997;18:286-291.

33. Cosman D, Fanger N, Borges L, et al. A novel immunoglobulin superfamily receptor for cellular and viral MHC class I molecules. Immunity. 1997;7:273-282.

34. Borges L, Hsu ML, Fanger N, Kubin M, Cosman D. A family of human lymphoid and myeloid Ig-like receptors, some of which bind to MHC class I molecules. J Immunol. 1997;159:5192-5196.

35. Cella M, Dohring C, Samaridis J, et al. A novel inhibitory receptor (ILT3) expressed on monocytes, macrophages, and dendritic cells involved in antigen processing. J Exp Med. 1997;185:1743-1751.

36. Samaridis J, Colonna M. Cloning of novel immunoglobulin superfamily receptors expressed on human myeloid and lymphoid cells: structural evidence for new stimulatory and inhibitory pathways. Eur J Immunol. 1997;27:660-665.

37. Wagtmann N, Rojo S, Eichler E, Mohrenweiser H, Long EO. A new human gene complex encoding the killer cell inhibitory receptors and related monocyte/macrophage receptors. Curr Biol. 1997;7:615-618.

38. Arm JP, Nwankwo C, Austen KF. Molecular identification of a novel family of human Ig superfamily members that possess immunoreceptor tyrosine-based inhibition motifs and homology to the mouse gp49B1 inhibitory receptor. J Immunol. 1997;159:2342-2349.

39. Pulford K, Micklem K, Thomas J, Jones M, Mason DY. A 72-kD B cell-associated surface glycoprotein expressed at high levels in hairy cell leukaemia and plasma cell neoplasms. Clin Exp Immunol. 1991;85:429-435.

40. Kremer EJ, Kalatzis V, Baker E, Callen DF, Sutherland GR, Maliszewski CR. The gene for the human IgA Fc receptor maps to 19q13.4. Hum Genet. 1992;89:107-108.

41. Meyaard L, Adema GJ, Chang C, et al. LAIR-1, a novel inhibitory receptor expressed on human mononuclear leukocytes. Immunity. 1997;7:283-290.

42. Colonna M, Nakajima H, Navarro F, Lopez-Botet M. A novel family of Ig-like receptors for HLA class I molecules that modulate function of lymphoid and myeloid cells. J Leukoc Biol. 1999;66:375-381.

43. Kim N, Takami M, Rho J, Josien R, Choi Y. A novel member of the leukocyte receptor complex regulates osteoclast differentiation. J Exp Med. 2002;195:201-209.

44. Merck E, Gaillard C, Gorman DM, et al. OSCAR is an FcR{gamma}-associated receptor expressed by myeloid cells, involved in antigen presentation and activation of human dendritic cells. Blood. 2004.

45. Aukhil I. Biology of wound healing. Periodontol 2000. 2000;22:44-50.

46. Lisitsyn N, Wigler M. Cloning the differences between two complex genomes. Science. 1993;259:946-951.

47. Sambrook J, Fritsch EF, Maniatis T. Molecular Cloning: a Laboratory Manual. Vol. 1 (ed 2nd). Cold Spring Harbor, NY: Cold Spring Harbor Laboratory Press; 1989.

48. Sambrook J, Fritsch EF, Maniatis T. Molecular Cloning: a Laboratory Manual. Vol. 1-3 (ed 2nd). Cold Spring Harbor, NY: Cold Spring Harbor Laboratory Press; 1989.

49. Sambrook J, Fritsch EF, Maniatis T. Molecular Cloning: a Laboratory Manual. Vol. 1 & 2 (ed 2nd). Cold Spring Harbor, NY: Cold Spring Harbor Laboratory Press; 1989.

50. Merck E, Gaillard C, Gorman DM, et al. OSCAR is an FcRgamma-associated receptor that is expressed by myeloid cells and is involved in antigen presentation and activation of human dendritic cells. Blood. 2004;104:1386-1395.

51. Walsh MC, Kim N, Kadono Y, et al. Osteoimmunology: interplay between the immune system and bone metabolism. Annu Rev Immunol. 2006;24:33-63.

52. Rho J, Takami M, Choi Y. Osteoimmunology: interactions of the immune and skeletal systems. Mol Cells. 2004;17:1-9.

53. Arron JR, Choi Y. Bone versus immune system. Nature. 2000;408:535-536.

54. Takayanagi H, Ogasawara K, Hida S, et al. T-cell-mediated regulation of osteoclastogenesis by signalling cross-talk between RANKL and IFN-[gamma]. Nature. 2000;408:600-605.

55. Takayanagi H, Kim S, Matsuo K, et al. RANKL maintains bone homeostasis through c-Fos-dependent induction of interferon-[beta]. Nature. 2002;416:744-749.

56. Li Q, Verma IM. NF-kappaB regulation in the immune system. Nat Rev Immunol. 2002;2:725-734.

57. Takashiba S, Van Dyke TE, Amar S, Murayama Y, Soskolne AW, Shapira L. Differentiation of Monocytes to Macrophages Primes Cells for Lipopolysaccharide Stimulation via Accumulation of Cytoplasmic Nuclear Factor kappa B. Infect Immun. 1999;67:5573-5578.

58. Ghosh S, May MJ, Kopp EB. NF- B AND REL PROTEINS: Evolutionarily Conserved Mediators of Immune Responses. Annual Review of Immunology. 1998;16:225-260.

59. Virca G, Kim S, Glaser K, Ulevitch R. Lipopolysaccharide induces hyporesponsiveness to its own action in RAW 264.7 cells. J Biol Chem. 1989;264:21951-21956.

60. Murthy PK, Dennis VA, Lasater BL, Philipp MT. Interleukin-10 Modulates Proinflammatory Cytokines in the Human Monocytic Cell Line THP-1 Stimulated with Borrelia burgdorferi Lipoproteins. Infect Immun. 2000;68:6663-6669.

61. Chen C-C, Wang J-K. p38 but Not p44/42 Mitogen-Activated Protein Kinase Is Required for Nitric Oxide Synthase Induction Mediated by Lipopolysaccharide in RAW 264.7 Macrophages. Mol Pharmacol. 1999;55:481-488.

62. Puren AJ, Fantuzzi G, Dinarello CA. Gene expression, synthesis, and secretion of interleukin 18 and interleukin 1beta are differentially regulated in human blood mononuclear cells and mouse spleen cells. PNAS. 1999;96:2256-2261.

63. Medvedev AE, Kopydlowski KM, Vogel SN. Inhibition of Lipopolysaccharide-Induced Signal Transduction in Endotoxin-Tolerized Mouse Macrophages: Dysregulation of Cytokine, Chemokine, and Toll-Like Receptor 2 and 4 Gene Expression. J Immunol. 2000;164:5564-5574.

64. Wahlstrom K, Bellingham J, Rodriguez JL, West MA. Inhibitory kappaBalpha control of nuclear factor-kappaB is dysregulated in endotoxin tolerant macrophages. Shock. 1999;11:242-247.

65. Maiuri MC, Tajana G, Iuvone T, et al. Nuclear factor-kappaB regulates inflammatory cell apoptosis and phagocytosis in rat carrageenin-sponge implant model. Am J Pathol. 2004;165:115-126.

66. Howell M, Borchers C, Milgram SL. Heterogeneous nuclear ribonuclear protein U associates with YAP and regulates its co-activation of Bax transcription. J Biol Chem. 2004;279:26300-26306.

67. Wu YH, Shih SF, Lin JY. Ricin triggers apoptotic morphological changes through caspase-3 cleavage of BAT3. J Biol Chem. 2004;279:19264-19275.

68. Kaltschmidt B, Kaltschmidt C, Hofmann TG, Hehner SP, Droge W, Schmitz ML. The pro- or anti-apoptotic function of NF-kappaB is determined by the nature of the apoptotic stimulus. Eur J Biochem. 2000;267:3828-3835.

69. Lin B, Williams-Skipp C, Tao Y, et al. NF-kappaB functions as both a proapoptotic and antiapoptotic regulatory factor within a single cell type. Cell Death Differ. 1999;6:570-582.

70. Hettmann T, DiDonato J, Karin M, Leiden JM. An essential role for nuclear factor kappaB in promoting double positive thymocyte apoptosis. J Exp Med. 1999;189:145-158.

71. Shishodia S, Aggarwal BB. Nuclear factor-kappaB: a friend or a foe in cancer? Biochem Pharmacol. 2004;68:1071-1080.

72. Graham FL, Smiley J, Russell WC, Nairn R. Characteristics of a human cell line transformed by DNA from human adenovirus type 5. J Gen Virol. 1977;36:59-74.

73. Verma IM, Stevenson JK, Schwarz EM, Van Antwerp D, Miyamoto S. Rel/NF-kappa B/I kappa B family: intimate tales of association and dissociation. Genes Dev. 1995;9:2723-2735.

74. Merck E, de Saint-Vis B, Scuiller M, et al. Fc receptor gamma-chain activation via hOSCAR induces survival and maturation of dendritic cells and modulates Toll-like receptor responses. Blood. 2005;105:3623-3632.

75. Kanehisa J, Yamanaka T, Doi S, et al. A band of F-actin containing podosomes is involved in bone resorption by osteoclasts. Bone. 1990;11:287-293.

76. Borges L, Kubin M, Kuhlman T. LIR9, an immunoglobulin-superfamily-activating receptor, is expressed as a transmembrane and as a secreted molecule. Blood. 2003;101:1484-1486.

77. Sather S, Kenyon KD, Lefkowitz JB, et al. A soluble form of the Mer receptor tyrosine kinase inhibits macrophage clearance of apoptotic cells and platelet aggregation. Blood. 2007;109:1026-1033.

78. Hubank M, Schatz DG. Identifying differences in mRNA expression by representational difference analysis of cDNA. Nucleic Acids Res. 1994;22:5640-5648.

79. Biassoni R, Pessino A, Bottino C, Pende D, Moretta L, Moretta A. The murine homologue of the human NKp46, a triggering receptor involved in the induction of natural cytotoxicity. Eur J Immunol. 1999;29:1014-1020.

80. Pessino A, Sivori S, Bottino C, et al. Molecular cloning of NKp46: a novel member of the immunoglobulin superfamily involved in triggering of natural cytotoxicity. J Exp Med. 1998;188:953-960.

81. Barten R, Torkar M, Haude A, Trowsdale J, Wilson MJ. Divergent and convergent evolution of NK-cell receptors. Trends Immunol. 2001;22:52-57.

82. Verfaillie T, Cox E, To LT, et al. Comparative analysis of porcine cytokine production by mRNA and protein detection. Vet Immunol Immunopathol. 2001;81:97-112.

83. Kim K, Kim JH, Lee J, et al. NFATc1 induces OSCAR gene expression during TRANCE-mediated osteoclastogenesis. J Biol Chem. 2005.

84. Kim Y, Sato K, Asagiri M, Morita I, Soma K, Takayanagi H. Contribution of NFATc1 to the transcriptional control of immunoreceptor OSCAR but not TREM-2 during osteoclastogenesis. J Biol Chem. 2005.

85. Lin L, Gerth AJ, Peng SL. Active Inhibition of Plasma Cell Development in Resting B Cells by Microphthalmia-associated Transcription Factor. J Exp Med. 2004;200:115-122.

86. Tsuchiya S, Kobayashi Y, Goto Y, et al. Induction of maturation in cultured human monocytic leukemia cells by a phorbol diester. Cancer Res. 1982;42:1530-1536.

87. Altman A, Isakov N, Baier G. Protein kinase Ctheta: a new essential superstar on the T-cell stage. Immunol Today. 2000;21:567-573.

88. Garcia A, Serrano A, Abril E, et al. Differential effect on U937 cell differentiation by targeting transcriptional factors implicated in tissue- or stage-specific induced integrin expression. Exp Hematol. 1999;27:353-364.

89. Merck E, Gaillard C, Scuiller M, et al. Ligation of the FcR gamma chain-associated human osteoclast-associated receptor enhances the proinflammatory responses of human monocytes and neutrophils. J Immunol. 2006;176:3149-3156.

90. Heaney ML, Golde DW. Soluble receptors in human disease. J Leukoc Biol. 1998;64:135-146.

91. Shiroishi M, Kajikawa M, Kuroki K, Ose T, Kohda D, Maenaka K. Crystal structure of the human monocyte-activating receptor, "Group 2" leukocyte Ig-like receptor A5 (LILRA5/LIR9/ILT11). J Biol Chem. 2006;281:19536-19544.

92. Koga T, Inui M, Inoue K, et al. Costimulatory signals mediated by the ITAM motif cooperate with RANKL for bone homeostasis. Nature. 2004;428:758-763.

93. Saverino D, Fabbi M, Ghiotto F, et al. The CD85/LIR-1/ILT2 inhibitory receptor is expressed by all human T lymphocytes and down-regulates their functions. J Immunol. 2000;165:3742-3755.

94. Ujike A, Takeda K, Nakamura A, Ebihara S, Akiyama K, Takai T. Impaired dendritic cell maturation and increased T(H)2 responses in PIR-B(-/-) mice. Nat Immunol. 2002;3:542-548.

95. Rudge EU, Cutler AJ, Pritchard NR, Smith KG. Interleukin 4 reduces expression of inhibitory receptors on B cells and abolishes CD22 and Fc gamma RII-mediated B cell suppression. J Exp Med. 2002;195:1079-1085.

96. Beinhauer BG, McBride JM, Graf P, et al. Interleukin 10 regulates cell surface and soluble LIR-2 (CD85d) expression on dendritic cells resulting in T cell hyporesponsiveness in vitro. Eur J Immunol. 2004;34:74-80.

97. Gomez-Lozano N, Estefania E, Williams F, et al. The silent KIR3DP1 gene (CD158c) is transcribed and might encode a secreted receptor in a minority of humans, in whom the KIR3DP1, KIR2DL4 and KIR3DL1/KIR3DS1 genes are duplicated. Eur J Immunol. 2005;35:16-24.

98. Willcox BE, Thomas LM, Chapman TL, Heikema AP, West AP, Jr., Bjorkman PJ. Crystal structure of LIR-2 (ILT4) at 1.8 A: differences from LIR-1 (ILT2) in regions implicated in the binding of the Human Cytomegalovirus class I MHC homolog UL18. BMC Struct Biol. 2002;2:6.

99. Willcox BE, Thomas LM, Bjorkman PJ. Crystal structure of HLA-A2 bound to LIR-1, a host and viral major histocompatibility complex receptor. Nat Immunol. 2003;4:913-919.

100. Martin AM, Kulski JK, Witt C, Pontarotti P, Christiansen FT. Leukocyte Ig-like receptor complex (LRC) in mice and men. Trends Immunol. 2002;23:81-88.

101. So H, Rho J, Jeong D, et al. Microphthalmia transcription factor and PU.1 synergistically induce the leukocyte receptor osteoclast-associated receptor gene expression. J Biol Chem. 2003;278:24209-24216.

102. Kim K, Lee J, Kim JH, et al. Protein inhibitor of activated STAT 3 modulates osteoclastogenesis by down-regulation of NFATc1 and osteoclast-associated receptor. J Immunol. 2007;178:5588-5594.

103. Kim K, Kim JH, Lee J, et al. MafB negatively regulates RANKL-mediated osteoclast differentiation. Blood. 2007;109:3253-3259.

104. Nakajima H, Asai A, Okada A, et al. Transcriptional regulation of ILT family receptors. J Immunol. 2003;171:6611-6620.

105. Tenca C, Merlo A, Merck E, et al. CD85j (leukocyte Ig-like receptor-1/Ig-like transcript 2) inhibits human osteoclast-associated receptor-mediated activation of human dendritic cells. J Immunol. 2005;174:6757-6763.

106. Kim GS, Koh JM, Chang JS, et al. Association of the OSCAR Promoter Polymorphism With BMDin Postmenopausal Women. J Bone Miner Res. 2005;20:1342-1348.

107. Moodie SJ, Norman PJ, King AL, et al. Analysis of candidate genes on chromosome 19 in coeliac disease: an association study of the KIR and LILR gene clusters. Eur J Immunogenet. 2002;29:287-291.

108. Kuroki S, Ikeda U, Maeda Y, Sekiguchi H, Shimada K. Lack of association between the insertion/deletion polymorphism of the angiotensin-converting enzyme gene and vasospastic angina. Clin Cardiol. 1997;20:873-876.

109. Wisniewski A, Luszczek W, Manczak M, et al. Distribution of LILRA3 (ILT6/LIR4) deletion in psoriatic patients and healthy controls. Hum Immunol. 2003;64:458-461.

110. Belkin D, Torkar M, Chang C, et al. Killer cell Ig-like receptor and leukocyte Ig-like receptor transgenic mice exhibit tissue- and cell-specific transgene expression. J Immunol. 2003;171:3056-3063.